2018

Modelling paralytic shellfish toxins (PST) accumulation in Crassostrea gigas by using Dynamic Energy Budgets (DEB)

Emilien Pousse
Ifremer, Institut Universitaire Europeen de la Mer, emilien.pousse@univ-brest.fr

Jonathan Flye-Sainte-Marie
Institut Universitaire Europeen de la Mer

Marianne Alunno-Bruscia
Ifremer

Helene Hegaret
IUEM, Institut Universitaire Europeen de la Mer

Eric Rannou
University of Brest, European University of Brittany

See next page for additional authors

Publication Details

Pousse, E., Flye-Sainte-Marie, J., Alunno-Bruscia, M., Hegaret, H., Rannou, E., Pecquerie, L., Marques, G. M., Thomas, Y., Castrec, J., Fabioux, C., Long, M.,Lassudrie, M., Hermabessiere, L., Amzil, Z., Soudant, P. & Jean, F. (2019). Modelling paralytic shellfish toxins (PST) accumulation in Crassostrea gigas by using Dynamic Energy Budgets (DEB). Journal of Sea Research, 143 152-164.

Modelling paralytic shellfish toxins (PST) accumulation in Crassostrea gigas by using Dynamic Energy Budgets (DEB)

Abstract

As other filter-feeders, Crassostrea gigas can concentrate paralytic shellfish toxins (PST) by consuming dinoflagellate phytoplankton species like Alexandrium minutum. Intake of PST in oyster tissues mainly results from feeding processes, i.e. clearance rate, pre-ingestive sorting and ingestion that are directly influenced by environmental conditions (trophic sources, temperature). This study aimed to develop a mechanistic model coupling the kinetics of PST accumulation and bioenergetics in C. gigas based on Dynamic Energy Budget (DEB) theory. For the first time, the Synthesizing Units (SU) concept was applied to formalize the feeding preference of oysters between non-toxic and toxic microalgae. Toxin intake and accumulation were both dependent on the physiological status of oysters. The accumulation was modelled through the dynamics of two toxin compartments: (1) a compartment of ingested but non-assimilated toxins, with labile toxins within the digestive gland eliminated via faeces production; (2) a compartment of assimilated toxins with a rapid detoxification rate (within a few days). Firstly, the DEB-PST model was calibrated using data from two laboratory experiments where oysters have been exposed to A. minutum. Secondly, it was validated using data from another laboratory experiment and from three field surveys carried out in the Bay of Brest (France) from 2012 to 2014. To account for the variability in PST content of A. minutum cells, the saxitoxin (STX) amount per energy units in a toxic algae (ρPST) was adjusted for each dataset. Additionally, the effects of PST on the oyster bioenergetics were calibrated during the first laboratory experiment. However, these effects were shown to depend on the strain of A. minutum. Results of this study could be of great importance for monitoring agencies and decision makers to identify risky conditions (e.g. production areas, seawater temperature), to properly assess detoxification step (e.g. duration, modalities) before any commercialization or to improve predictions regarding closing of shellfish areas.

Publication Details

Pousse, E., Flye-Sainte-Marie, J., Alunno-Bruscia, M., Hegaret, H., Rannou, E., Pecquerie, L., Marques, G. M., Thomas, Y., Castrec, J., Fabioux, C., Long, M.,Lassudrie, M., Hermabessiere, L., Amzil, Z., Soudant, P. & Jean, F. (2019). Modelling paralytic shellfish toxins (PST) accumulation in Crassostrea gigas by using Dynamic Energy Budgets (DEB). Journal of Sea Research, 143 152-164.

Authors

Emilien Pousse, Jonathan Flye-Sainte-Marie, Marianne Alunno-Bruscia, Helene Hegaret, Eric Rannou, Laure Pecquerie, Goncalo M. Marques, Yoann Thomas, Justine Castrec, Caroline Fabioux, Marc Long, Malwenn Lassudrie, Ludovic Hermabessiere, Zouher Amzil, Philippe Soudant, and Fred Jean

Modelling paralytic shellfish toxins (PST) accumulation in *Crassostrea gigas* by using Dynamic Energy Budgets (DEB)

Émilien Pousse[a,b], Jonathan Flye-Sainte-Marie[a], Marianne Alunno-Bruscia[b], Hélène Hégaret[a], Éric Rannou[d], Laure Pecquerie[a], Gonçalo M. Marques[e], Yoann Thomas[a], Justine Castrec[a], Caroline Fabioux[a], Marc Long[a,f], Malwenn Lassudrie[a], Ludovic Hermabessiere[a], Zouher Amzil[c], Philippe Soudant[a], Fred Jean[a]

[a] *Laboratoire des Sciences de l'Environnement Marin LEMAR-UMR6539, Institut Universitaire Européen de la Mer, Université de Bretagne Occidentale, Place Copernic, Technopôle Brest-Iroise, 29280 Plouzané, France*
[b] *Ifremer, UMR 6539 LEMAR, 11 presqu'île du Vivier, 29840 Argenton-en-Landunvez, France*
[c] *Ifremer, Laboratoire Phycotoxines, rue de l'Ile d'Yeu, BP 21105, F-44311 Nantes, France*
[d] *Université Européenne de Bretagne, Université de Brest ; UMR 6205 Laboratoire de Mathématiques ; 6 avenue Le Gorgeu, C.S. 93837, 29238 Brest Cedex 3, France*
[e] *MARATEC–Marine, Environment and Technology Center, Instituto Superior Técnico, Universidade de Lisboa, Avenida Rovisco Pais 1, 1049-001 Lisboa, Portugal*
[f] *School of Chemistry, University of Wollongong, NSW 2522, Australia*

Abstract

As other filter-feeders, *Crassostrea gigas* can concentrate paralytic shellfish toxins (PST) by consuming dinoflagellate phytoplankton species like *Alexandrium minutum*. Intake of PST in oyster tissues mainly results from feeding processes, i.e. clearance rate, pre-ingestive sorting and ingestion that are directly influenced by environmental conditions (trophic sources, temperature). This study aimed to develop a mechanistic model coupling the kinetics of PST accumulation and bioenergetics in *C. gigas* based on Dynamic Energy Budget (DEB) theory. For the first time, the Synthesizing Units (SU) concept was applied to formalize the feeding preference of oysters between non-toxic and toxic microalgae. Toxin intake and accumulation were both dependent on the physiological status of oysters. The accumulation was modelled through the dynamics of two toxin compartments: (1) a compartment of ingested but non-assimilated toxins, with labile toxins within the digestive gland eliminated *via* faeces production; (2) a compartment of assimilated toxins with a rapid detoxification rate (within a few days). Firstly, the DEB-PST model was calibrated using data from two laboratory experiments where oysters have been exposed to *A. minutum*. Secondly, it was validated using data from another laboratory experiment and from three field surveys carried out in the Bay of Brest (France) from 2012 to 2014. To account for the variability in PST content of *A. minutum* cells, the saxitoxin (STX) amount per energy units in a toxic algae (ρ_{PST}) was adjusted for each dataset. Additionally, the effects of

PST on the oyster bioenergetics were calibrated during the first laboratory experiment. However, these effects were shown to depend on the strain of *A. minutum*. Results of this study could be of great importance for monitoring agencies and decision makers to identify risky conditions (*e.g.* production areas, seawater temperature), to properly assess detoxification step (*e.g.* duration, modalities) before any commercialization or to improve predictions regarding closing of shellfish areas.
Keywords: *Alexandrium minutum*, Paralytic shellfish toxins (PST), Dynamic Energy Budget (DEB), Modelling, Pacific oyster

1. Introduction

Proliferating phytoplankton species can cause damages to other marine organisms by modifying the environment (i.e. eutrophication, foams production, depletion of oxygen, destruction of habitats) or by synthesizing toxins that can be accumulated in the trophic web (Anderson et al., 2002). Dinoflagellate belonging to the genus *Alexandrium* are responsible for most paralytic shellfish poisoning (PSP) events. In 1994, the first human cases of PSP due to a bloom of *Alexandrium* sp. were reported in the Mediterranean sea (Honsell et al., 1996). Since then, this genus has been increasingly incriminated for other events worldwide (Anderson, 1989; Hallegraeff, 1993; Cembella, 1998; Guallar et al., 2017). *A. minutum* synthesizes paralytic shellfish toxins (PST), including STX and its derivatives, that can be bioaccumulated throughout the food chain *via* feeding. Filter-feeders, such as bivalves, are primary consumers and are able to bioaccumulate these toxins. At high concentrations, PST can have deleterious effects on the immune response and homoeostasis of bivalves, and are responsible for myoatrophies, alterations of the digestive gland or of other tissues (Haberkorn et al., 2010a,b; Hégaret et al., 2012). Moreover, by accumulating high loads of these toxins, filter-feeders may also become toxic for secondary consumers, including humans, by provoking tingling, numbness, paralysis and death by respiratory arrest (Shumway, 1990) in the worst case. Many countries have established monitoring programs in order to limit the risk of human intoxication (Visciano et al., 2016). In Europe for instance, above the threshold of 80 µg STX 100 g^{-1} of shellfish tissues, the commercialization and harvesting of bivalves is closed, which induces economical losses for shellfish producers.

Different toxicokinetics (TK) models have been proposed to describe the kinetics of PST accumulation and detoxification in bivalves by modelling either ingestion processes or toxin biotransformation (*e.g.*

∗. Email : flye@univ-brest.fr

Yamamoto et al., 2003; Lassus et al., 2004, 2007; Guéguen et al., 2011). In *Crassostrea gigas*, the accumulation of PST is influenced by the oyster feeding (Pousse et al., 2017), which is directly linked to the seawater temperature (Bougrier et al., 1995), the food availability (Barillé et al., 1993) and the physiological status of the animal (Soletchnik et al., 1997). Thus, in order to better understand and predict the relationships between the environment, the individual physiology and the toxin accumulation, there is a need to couple a bioaccumulation model to an individual physiological model.

A bioenergetic model based on Dynamic Energy Budgets (DEB) theory has been developed and used for *C. gigas* (*e.g.* Pouvreau et al., 2006; Bourlès et al., 2009; Alunno-Bruscia et al., 2011; Bernard et al., 2011; Thomas et al., 2016; Gourault et al., 2018). DEB theory describes and quantifies the energy flows from ingestion and assimilation to maintenance, growth, maturation and reproduction of an individual (Kooijman, 2010). For two marine fishes, the hake and the sole (Bodiguel et al., 2009; Eichinger et al., 2010) and two mussels (Van Haren et al., 1994; Casas and Bacher, 2006), realistic TK models based on DEB enabled to predict the concentration of xenobiotics in the animal tissues by coupling bioaccumulation and detoxification of xenobiotics to energy flows. However, these previous studies did not integrate the direct effects of contaminants on organisms as is aimed at by toxicodynamics models (TD). To address this last issue the DEBtox framework has been developed in the context of DEB theory (Kooijman and Metz, 1984; Kooijman and Bedaux, 1996; Jager and Zimmer, 2012). A DEB-based TKTD approach dealing with PST bioaccumulation and including sub-lethal bioenergetics impacts on *C. gigas* (Li et al., 2002; Haberkorn et al., 2010a,b) would thus be very promising.

The synthesizing units (SU) concept, compatible with DEB theory, was shown to be able to account for the trophic preference of bivalves (Kooijman, 1998, 2006, 2010; Saraiva et al., 2011; Lavaud et al., 2014). Oysters are able to sort the particles they ingest (Ward and Shumway, 2004) when they are exposed to a mixture of algae, including toxic and non-toxic ones. Although the pre-ingestive sorting in bivalves relies on the size, the nutritive quality and/or the carbohydrate signature of algae (Ward et al., 1998; Rosa et al., 2013; Espinosa et al., 2016; Rosa et al., 2017a), rather than on intracellular toxins such as PST (Li and Wang, 2001), this process may also affect the toxin accumulation (Mafra et al., 2009). Thus, the concept of SUs (Kooijman, 1998) is potentially useful to assess specifically the quantity of toxic algae consumed by an oyster when exposed to a mix of toxic and non-toxic algae.

The aim of this work was to describe the bioaccumulation kinetics of PST in *C. gigas* and to integrate the effects of these toxins in the oyster-DEB model. Firstly, we calibrated a DEB model describing PST

accumulation from datasets collected under laboratory controlled conditions that combine data on oyster growth, toxin content and detoxification. Secondly, the model was validated with data from independent laboratory experiment and from field surveys conducted in the bay of Brest (Brittany, France) in 2012, 2013 and 2014.

2. Material and methods

2.1. Model formalization

2.1.1. Oyster DEB model

PST kinetics and effects were coupled/integrated in a Dynamic Energy Budget model (Fig. 1). We based our model development on an existing and already published DEB model for *C. gigas*. This allowed us to quantify the dynamics of the energy budget of the oyster. This model is derived from a standard DEB model described by Kooijman (2000, 2010) and first applied to this species by Pouvreau et al. (2006). The model equations are those of Bernard et al. (2011). As the purpose of this study was not to address the process of spawning and more generally oyster gametogenesis, for the sake of simplification, energy fluxes linked to the gonad defined in Bernard et al. (2011) and further applied by Thomas et al. (2016) were not integrated within this model. The conceptual scheme of the model and the equations are given in Fig. S1 and Tab. S1 of Appendix 1 in Supplementary material, respectively. Further explanations about the model principles are given in Appendix 1 in Supplementary material. The parameter set used in this study is that used by Thomas et al. (2016), only one parameter value has been modified to allow the model to describe control (without toxic algae) observations: the size at puberty (L_{wp} here considered as a fixed value according to Kooijman, 2000). Parameters are given in Tab. S2 of Appendix 2.

2.1.2. Toxin intake

PST toxins (saxitoxins and analogues) are mainly intracellular (Yasumoto and Murata, 1993; Hallegraeff et al., 2003). Consequently, the main accumulation pathway within the food chain occurs with ingestion by algal consumers. In the presence of both toxic and non-toxic algae, oysters are able to select one type of algae, which may affect toxin accumulation (Mafra et al., 2009). This selection phenomenon relies on complex mechanisms of pre-ingestive sorting (Ward et al., 1998) and controls toxic algae ingestion rate: in the presence of a specific toxic algae concentration, toxic algae ingestion rate is dependent upon the presence and concentration of non toxic algae. The synthesizing units (SU) concept (Kooijman, 1998) has been used to account for this selection in bivalves in accordance with Saraiva et al. (2011) and Lavaud et al. (2014). In

the present study, we distinguished only two food sources: non-toxic and toxic algae (respectively denoted N and T). The preference formulation was taken from Lavaud et al. (2014). The SU scheme was based on substitutable substrates that bind in a sequential way (Kooijman, 2010). A SU binds to a substrate (either N or T) with a maximum binding rate ($\{\dot{F}_{Nm}\}$ and $\{\dot{F}_{Tm}\}$, respectively) and unbinds with a maximum dissociation rate $\{\dot{h}_{Am}\}$. When a non-toxic alga (N) arrives while the SU is bound to a toxic alga (T), the SU can unbind from T to bind with N. The rate at which a SU substitutes a toxic alga to a non-toxic alga is denoted $\dot{b}_{NT}$. Theoretically, the reverse (substituting a non-toxic alga to a toxic alga) is also possible but this possibility was ignored given the low preference of *C. gigas* for species in the *Alexandrium* genus (Espinosa et al., 2016; Pousse et al., 2017). Parameters, symbols and units of this SU system are summarized in Table 1. According to Lavaud et al. (2014), the functional responses for non-toxic (f_N) and toxic (f_T) substrates are written as follows:

$$f_N = \frac{\alpha_T \{\dot{F}_{Nm}\} N - \beta_N \{\dot{F}_{Tm}\} T}{\alpha_N \alpha_T - \beta_N \beta_T} \tag{1a}$$

$$f_T = \frac{\alpha_N \{\dot{F}_{Tm}\} T - \beta_T \{\dot{F}_{Nm}\} N}{\alpha_N \alpha_T - \beta_N \beta_T} \tag{1b}$$

with:

$$\alpha_N = \{\dot{h}_{N\,Am}\} + \{\dot{F}_{Nm}\} N; \quad \alpha_T = \{\dot{h}_{T\,Am}\} + \{\dot{F}_{Tm}\} T + \dot{b}_{NT} N \tag{2a}$$

$$\beta_N = \{\dot{F}_{Nm}\} N - \dot{b}_{NT} N; \quad \beta_T = \{\dot{F}_{Tm}\} T \tag{2b}$$

where $\{\dot{F}_{Nm}\}$ and $\{\dot{F}_{Tm}\}$ are respectively the binding rates ($L\,d^{-1}\,cm^{-2}$) of non-toxic and toxic algae, $\{\dot{h}_{N\,Am}\}$ and $\{\dot{h}_{T\,Am}\}$ the dissociation rates ($cell\,d^{-1}\,cm^{-2}$) of non-toxic and toxic algae, $\dot{b}_{NT}$ the binding rates ($L\,d^{-1}\,cm^{-2}$) of non-toxic algae from toxic algae. The dissociation rates can be calculated according to Lavaud et al. (2014):

$$\{\dot{h}_{N\,Am}\} = \frac{\{\dot{p}_{Xm}\} \kappa_{X_N}}{\rho_E\, w_E\, y_{EN}\, M_N} \tag{3a}$$

$$\{\dot{h}_{T\,Am}\} = \frac{\{\dot{p}_{Xm}\} \kappa_{X_T}}{\rho_E\, w_E\, y_{ET}\, M_T} \tag{3b}$$

with $\{\dot{p}_{Xm}\}$ the oyster maximum surface-specific ingestion rate ($J\,d^{-1}\,cm^{-2}$), κ_{X_N} and κ_{X_T} the assimilation efficiency for non-toxic and toxic algae, w_E the molecular weight of reserve, ρ_E the scaled energy content of reserve ($J\,{g_{dw}}^{-1}$), y_{EN} and y_{ET} the yields of reserve from non-toxic and toxic algae ($g_{dw}\,{g_{dw}}^{-1}$), M_N and M_T the dry mass of non-toxic and toxic algae, respectively.

Ingestion rate $\dot{p}_X$ ($J\,d^{-1}$) is equal to the sum of the ingestion of non-toxic and toxic algae and depends on the oyster structural surface-area ($V^{2/3}$; Kooijman, 2010). It can be written as:

$$\dot{p}_X = \{\dot{p}_{Xm}\}\, V^{2/3} (\, f_N + f_T\,) \tag{4}$$

The flux of ingested toxins ($\dot{J}_{X_{PST}}$, $\mu g\, STX\, eq.\, d^{-1}$), that is proportional to toxic algae ingestion rate, can be described as:

$$\dot{J}_{X_{PST}} = \{\dot{p}_{Xm}\}\, V^{2/3}\, f_T\, \rho_{PST} \tag{5}$$

with ρ_{PST}, the PST amount per energy unit in toxic algae ($\mu g STX\, eq.\, J^{-1}$). This parameter varies with cellular toxicity which is known to depend on algal strain and/or growth conditions (Chou et al., 2004; Leong et al., 2004).

2.1.3. Toxin dynamics

A fraction of the ingested toxic algae is assimilated (or absorbed, i.e. enters in the oyster body) in oyster tissues while the other fraction is egested through the gut whithout being assimilated (Laabir et al., 2007; Hégaret et al., 2008). Dynamics and processes of elimination are very different if toxins are assimilated (elimination through detoxification) or not (elimination by egestion). For this reason, PST dynamics need to be described by two compartments (Silvert and Cembella, 1995; Yamamoto et al., 2003; Lassus et al., 2007): a compartment of unassimilated toxins, that is characterized by a short-term turnover (within a few hours), and a compartment of assimilated toxins with a mid-term turnover (several weeks). A schematic representation of these two compartments is given in Fig.1. Despite the fast dynamics, the gut toxin content can represent an important proportion of the total bivalve toxin content (Bricelj et al., 1990; Kwong et al., 2006) and cannot be neglected.

Unassimilated toxins compartment. PST enter this compartment through ingestion and leave through either assimilation or egestion. The dynamics of unassimilated toxins (Q_U) can thus be written as:

$$\frac{d}{dt} Q_U = \dot{J}_{X_{PST}} - \dot{J}_{A_{PST}} - \dot{J}_{E_{PST}} \tag{6}$$

where $\dot{J}_{X_{PST}}$, $\dot{J}_{A_{PST}}$ and $\dot{J}_{E_{PST}}$ are respectively the ingestion, assimilation and egestion rates of toxins. For parsimony purposes, the digestive tract was considered as a simple plug-flow system in which assimilation of toxins occurs immediately after ingestion and at a constant efficiency ($\kappa_{X_{PST}}$). Because the toxin digestion differs from processes associated to edible food (*e.g.* involvement of an immune response), we considered

this value to be different from the assimilation efficiency κ_X. The parameter values, symbols and units used to model PST dynamics are summarized in Table 1. The toxin assimilation rate was thus written as:

$$\dot{J}_{A_{PST}} = \dot{J}_{X_{PST}} \kappa_{X_{PST}} \tag{7}$$

According to Kooijman (2010), the gut transit time (t_g) is considered to be proportional to structural length ($V^{1/3}$). The toxin egestion rate at time t is taken to be equal to the toxin ingestion rate at time $t - t_g$ minus toxin assimilation rate at time $t - t_g$:

$$\dot{J}_{E_{PST}}(t) = \dot{J}_{X_{PST}}(t - t_g) - \dot{J}_{A_{PST}}(t - t_g) \tag{8}$$

Assimilated toxins compartment. PST enter this compartment through assimilation ($\dot{J}_{A_{PST}}$) and only leave through detoxification ($\dot{J}_{elim_{PST}}$; Cembella et al., 1994; Oshima, 1995; Navarro and Contreras, 2010). Because gametes only contain less than 3 % of the total toxin content of the oyster (Hégaret et al., unpublished data), we assumed that spawning is not associated to toxin release. Dynamics of assimilated toxins (Q_A) thus amounts to:

$$\frac{d}{dt} Q_A = \dot{J}_{A_{PST}} - \dot{J}_{elim_{PST}} \tag{9}$$

The elimination rate is proportional to Q_A through an elimination rate constant (k_{elim}, in d^{-1}):

$$\dot{J}_{elim_{PST}} = k_{elim}\, Q_A \tag{10}$$

Total concentration in toxins. In order to compare the model predictions with observations, the total concentration in toxins ($[PST]_w$, µg STX eq. $100\mathrm{g}^{-1}$ of wet flesh mass) was calculated as:

$$[PST]_w = \frac{Q_U + Q_A}{W_w} \times 100 \tag{11}$$

with Q_A and Q_U the contents of the two toxin compartments, and W_w the wet flesh mass of the oyster predicted by the DEB model (see Appendix 1 for detailed computation of W_w).

2.1.4. Effects of PST on oysters

In *C. gigas*, PST induce alterations in tissues (Haberkorn et al., 2010b; Hégaret et al., 2012), an immune response (Haberkorn et al., 2010a), detoxification processes (Rolland et al., 2014) or prevention mechanisms of cellular damages (Rolland et al., 2014; Fabioux et al., 2015). To model the effects of toxins upon oyster bioenergetics, we assumed that PST increases the somatic maintenance costs. Because oyster responses have been observed during presence of unassimilated *A. minutum* cells in the intestine (encapsulation), both

assimilated and unassimilated toxin compartments have been assumed to contribute to this increase. These effects have been modelled according to the DEBtox rules (Kooijman and Bedaux, 1996; Jager et al., 2014): when the no-effect concentration ($[PST]_{NEC}$) is exceeded (Jager and Zimmer, 2012), a toxicant stress parameter ($[PST]_q$) allows one to linearly scale the impact of PST as a function of the total concentration of PST ($[PST]_w$). The volume specific somatic maintenance cost ($[\dot{p}_M]$; $J\,cm^{-2}\,d^{-1}$) can be written as:

$$[\dot{p}_M] = [\dot{p}_{M_0}] + [\dot{p}_{M_0}] \frac{1}{[PST]_q} max(0, [PST]_w - [PST]_{NEC}) \quad (12)$$

with $[\dot{p}_{M_0}]$, the volume-specific somatic maintenance cost in the absence of toxins ($J\,cm^{-3}\,d^{-1}$).

2.2. Datasets

Parameters of the DEB-PST model (Tab. 1 and S2) were estimated by minimizing squared deviation between the mean of observations (originated from datasets 1 and 2) and the mean of model predictions. To assess the influence of the estimated parameters, a sensitivity analysis was carried out (Appendix 3, Fig. S2). Then, the model with its parameters set was validated by comparing model predictions and observations from two independent datasets with different *A. minutum* strains and different conditions of exposures to *A. minutum* (laboratory or field; datasets 3 and 4 respectively). Main information of the datasets are summarized in Table 2.

Datasets 1 and 2 (parameters calibration)

Dataset 1. The food ingestion, the toxin accumulation and the growth of 3-month old oysters (total wet mass = 2.3 g ± 0.9; see Petton et al., 2013) were measured over 6 or 8 weeks under 4 different trophic conditions: (1) no food for 8 weeks; (2) a 6-weeks diet with non-toxic algae exclusively; (3) a 6-weeks diet composed by non-toxic and toxic algae; (4) a 2-weeks diet of non-toxic and toxic algae, followed by no food for 6 weeks (Table 2).

Three triplicate 50-L tanks per condition with a biomass of 300 g oysters (120 animals) were supplied with 1-µm filtered and UV-treated seawater at a constant flow of 120 $mL\,min^{-1}$ and at a temperature of 21°C. In conditions 2, 3 and 4, the non-toxic phytoplankton diet consisted in *Tisochrysis lutea* (CCAP 927/14) and *Chaetoceros muelleri* (CCAP 1010/3) in equal biomass proportion. The non-toxic algae were continuously distributed in the tanks so that the outflow concentration was kept between 1000 and 2000 $\mu m^3\ \mu L^{-1}$ ($\approx\ 2.5\,10^7\,cell\,L^{-1}$). In conditions 3 and 4, the toxic algae *A. minutum* (strain Daoulas 1257 RCC4876, isolated in Brittany) was added to the non-toxic algae at a concentration varying from $2\,10^5$ to

$6.5\,10^5$ cell L^{-1} (see Pousse et al., 2017). This strain with almost no bioactivity of extracellular compounds (quantified by an allelopathic assay directed towards a diatom species, Long et al., 2018) was chosen to study the impact of PST on oysters. PST profile of this strain (45% C2, 22% C1, 21% GTX3, 12% GTX2, in mole %) was quantified by HPLC-FLD at Ifremer PHYC laboratory (Nantes, France) according to the method described in Oshima (1995) with adaptations from Guéguen et al. (2011). A PST concentration of 0.053 pg STX-diHCl eq. $cell^{-1}$ was calculated with EFSA toxicity equivalency factors (EFSA, 2009).

In each tank, 20 individuals were sampled weekly (except in weeks 5 and 7 for conditions 1 and 4), measured (shell length, mm) and weighed (total wet mass and wet flesh mass, g, precision of 10^{-3} g). The dry flesh mass was estimated on 10 individuals, PST were quantified on 5 animals of conditions 3 and 4 (the 5 remaining oysters were used for a histological survey, data not shown). In condition 3, 5 oysters experienced a 6-days detoxification step in filtered seawater at the end of the 6-week diet of toxic and non-toxic algae. In condition 4, 2 individuals per tank were sampled on days 1, 2, 3, 4, 5, 7, 9, 11 and 13 of the detoxification step to measure PST content and estimate toxin elimination kinetics.

The concentrations of PST in oysters were quantified by using ELISA PSP kit developed by Abraxis (see methods in Lassudrie et al., 2015a,b). Oyster tissues were mixed in pools of 5 individuals (1:1, mass:volume) in 0.1 M HCl solution, grounded (Fastprep-24 5G homogenizer) and boiled for 5 min at 100°C in order to acid-hydrolyze some PST analogs into saxitoxin (STX), neoSTX and GTX1-4. The samples were then analyzed with the Abraxis ELISA PSP kit following the manufacturer instructions and toxin concentrations were estimated by spectrophotometry and expressed as µg of STX eq. for 100 g of total flesh mass.

Dataset 2. We used initial individual mass (in dry flesh mass) and toxin concentrations data of oysters that were exposed for 2 days to non-toxic algae and then for 2 days to *A. minutum* (for a detailed description see Pousse et al., 2017).

Datasets 3 and 4 (model validation)

Dataset 3. Adult oysters (mean wet flesh mass = 2.44 g ± 0.57) were conditioned during 8 weeks under a mixed diet of non-toxic (*T. lutea* and *C. muelleri*) and toxic (*A. minutum*) algae. Non-toxic algae were distributed to maintain a concentration ranging between 1000 and 2000 μm^3 μL^{-1} in the tank outflow; meanwhile *A. minutum* was distributed at a concentration of 10^5 *cell* L^{-1}. During the penultimate week of conditioning, the concentration of *A. minutum* was raised to $5\,10^5$ cell L^{-1} on days 1 and 4 and 10^6 cell L^{-1} on days 2 and 3 to simulate a bloom of *A. minutum*. The strain of *A. minutum* used in this experiment (AM89BM RCC1490) was isolated in the bay of Morlaix (Brittany, France) in 1995 and synthesized 1.3

pg STX-diHCl eq. cell^{-1} (40% GTX3, 9% GTX2, 30% C2, 20% C1, ≈ 1% dc-GTX2 and dc-GTX3 in %mole). This strain also produces extracellular compounds known to have allelopathic and cytotoxic effects on other algae and marine organisms (Lelong et al., 2011; Borcier et al., 2017; Castrec et al., 2018). For this experiment, PST concentrations were measured in the oyster digestive gland with the ELISA method. They were further corrected to take into account the mass of the digestive gland and the ratio of PST in this organ compared to the whole body (Guéguen, 2009).

Dataset 4. We used data of the Bay of Brest where recurrent blooms of *A. minutum* have been monitored (Chapelle et al., 2015). From 2012 to 2014, oysters were transferred at Pointe du Chateau (48°20'03"N, 04°19'145"W) in June or July when concentrations of *A. minutum* were expected to increase. When a bloom occurred, oysters were sampled regularly in order to monitor the PST concentration in their tissues. In July 2012 during a bloom of *A. minutum*, two oyster groups were transferred into the laboratory at a week interval, in order to monitor their detoxification in filtered seawater over 1 week. Concentrations of *A. minutum* were obtained from seawater samples collected biweekly on the site where oysters were located. Enumeration of non-toxic algae were quantified weekly. Seawater temperature was measured by the monitoring network SOMLIT (http://somlit-db.epoc.u-bordeaux1.fr/bdd.php). After linear interpolation, algae enumerations and seawater temperature were used as forcing variables for the DEB-PST model. In addition, PST content of *A. minutum* was monitored during the 2013 bloom and quantified in the PHYC laboratory of Nantes (see Guéguen et al., 2011, for the method). PST concentrations in the oyster digestive glands were measured individually with ELISA assay or by HPLC-FLD (Oshima, 1995) for the 2012 survey (see toxin profiles in Appendix 4.2, Tab. S3). The calibration curve between these two techniques (Appendix 4.2, Fig. S3) were plotted and applied on HPLC-FLD data so that data could be compared. These concentrations have also been corrected to be expressed as a function of the total wet flesh mass of oysters.

2.3. Model predictions and inter-individual variability

Both growth and toxin accumulation are known to vary among individuals. To take into account this variability, the simulated individuals differed in initial conditions (V, E and E_R) and in clearance rate as explained hereafter.

2.3.1. Initial conditions

Based upon observations of length (L_w) and dry mass (W_d), initial conditions were calculated as: $V = (L_w\,\delta_M)^3$, $E = e\,[E_m]\,V$, $E_R = 0$ in juveniles and $E_R = (W_d - V\,d_V)\rho_E - E$ in adults. Parameter significance

and values are given in Tab. S3. The scaled reserve density (e) was taken to vary seasonally and was fixed to 0.2 for dataset 1 (November), 0.5 for datasets 2 and 3 (March and April respectively) and 0.7 for dataset 4 (July). Missing data of W_d and L_w during the 2012 survey (dataset 4) led to compensate by simulating 20 individuals ranging from 0.1 to 2 g in dry flesh mass (range observed for 2013 survey) and length was estimated from the dry flesh mass.

2.3.2. Clearance rates

The individual accumulation potential of oysters was shown to be closely related to the individual clearance rate so that animals could be clustered into three groups with low, intermediate, and high toxin accumulation potential (Pousse et al., 2017). Accordingly, individuals were respectively distributed in these clusters with the following frequencies: 25 %, 50 % and 25 %. One of these three groups was thus attributed randomly to each individual in accordance with the frequencies given above. Based upon the clearance rates measured in Pousse et al. (2017) (dataset 2), individuals with a low potential for PST accumulation had binding rates on non-toxic algae ($\{\dot{F}_{Nm}\}$) and toxic algae ($\{\dot{F}_{Tm}\}$) equal to 12 and 1.5 $\mathrm{L\,d^{-1}\,cm^{-2}}$; intermediate to 16 and 4 $\mathrm{L\,d^{-1}\,cm^{-2}}$ and high to 20 and 8 $\mathrm{L\,d^{-1}\,cm^{-2}}$, respectively. This method of including inter-individual variability was applied to the data from Pousse et al. (2017). Based upon *A. minutum* concentrations in each trial, the PST concentrations measured in oyster tissues by Pousse et al. (2017) were compared to the PST concentrations predicted by the DEB-PST model.

3. Results

3.1. Parameter estimation

3.1.1. Oyster DEB-model

Based upon the growth observations of oysters exposed to conditions 1 and 2 of the dataset 1 (Fig. 2, A, B), values of 0.05 $\mathrm{g_{dw}\,g_{dw}^{-1}}$ for y_{EN} and 0.79 for κ_{LR} were estimated. These values represent a satisfactory estimation of oyster growth in both conditions. Unfortunately, it was impossible for us to estimate κ_{LV} (yield of structure tissue used for maintenance) as the starvation was not strong enough to induce a structure lysis. Its value was arbitrary fixed to 0.79. All parameters values are summarized in Tables 1 and S2.

3.1.2. Accumulation model

The PST accumulation in oysters of the condition 3 (dataset 1, *A. minutum* mixed with other non-toxic algae for 6 weeks) was rather low (highest concentration = 14.9 µg STX eq. $\mathrm{100g^{-1}}$; Fig. 3, A).

A value of 0.18 was estimated for PST assimilation efficiency $\kappa_{X_{PST}}$ from this dataset. Algal cell counts in water inflow and outflow indicated that the feeding rates of oysters were highly variable from day to day, presumably because of variations in quality of the non-toxic algae. To account for this variability, the parameters $\{\dot{F}_{Nm}\}$ and $\{\dot{F}_{Tm}\}$ were corrected in accordance with observations of ingestion measured daily in the experimental tanks. Although the model overestimated PST accumulation at the first and third sampling points, predictions were generally in good agreement with observations (Fig. 3, A). First-order kinetics for toxin elimination with a value of 0.17 d^{-1} for k_{elim} enabled us to describe accurately the toxin dynamics in condition 4 (dataset 1; Fig. 3, B). From dataset 2 with *A. minutum* as single algae supply, a value of 0.005 $g_{dw}\, g_{dw}^{-1}$ was estimated for y_{ET} (yield of reserve from toxic algae).

By combining the results from datasets 1 (Fig. 3) and 2 (Fig. 4), in which the same *A. minutum* strain was used, a value of 0.130 $\mu g STX\,eq.\,J^{-1}$ was adjusted for the STX amount per energy unit in a toxic particle (ρ_{PST}) for this strain.

3.1.3. Inter-individual variability

The capacity of the model to predict realistic variability in toxin bio-accumulation based upon the variability in oyster clearance rate was validated on data from Pousse et al. (2017) (dataset 2). Based upon the three mean values of clearance rate measured for the three oyster groups with low, intermediate, or high accumulation potential in (Pousse et al., 2017), we observed a rather good fit of the predicted PST concentrations in oysters compared to those observed ($r^2 = 0.78$, Fig. 4).

3.1.4. Effects induced by PST

Without taking into account the PST effects on the maintenance costs, the model allowed us to predict properly the gain and loss in mass of oysters for conditions 3 and 4 (dataset 1, Fig. 5; dashed lines). Nevertheless, in condition 4 (B), the model slightly overestimated observations. Deleterious effects of PST upon oysters were included by setting $[PST]_{NEC} = 0.1\ \mu g\,STX\,eq.\,100g^{-1}$ and $[PST]_q = 7\ \mu g\,STX\,eq.\,100g^{-1}$ which allowed us to improve the model predictions of oyster growth (Fig. 5 A; continuous line) although the mass loss was still slightly underestimated once oysters had totally depurated (Fig. 5 B; continuous line).

3.2. Model validation

3.2.1. Laboratory experiment (dataset 3)

The ρ_{PST} value adjusted with previous experiments (datasets 1 and 2) did not allow us to obtain a good fit with observations of bioaccumulation in dataset 3. However, PST cellular toxicity of the *A. minutum*

strain used in this experiment is known to be an order of magnitude higher than for the strain used in datasets 1 and 2 (Castrec et al., 2018). Increasing the value of ρ_{PST} by a factor 1.15 produced a better fit of the model with observations (Fig. 6; A). The growth of oysters was also properly predicted, although the mass loss at the end of the experiment was underestimated (Fig. 6 B; black continuous line). The *A. minutum* strain used in this experiment is also known to produce extracellular compounds which might contribute to toxicity (Borcier et al., 2017; Castrec et al., 2018) and affect energy balance. Taking into account this higher toxicity by decreasing toxicant stress concentration ($[PST]_q$) to 1 µg STX eq. $100g^{-1}$ (the lower the value of $[PST]_q$, the higher the PST effects) provided a better fit between the predictions and the observations (Fig. 6 B, black dashed line).

3.2.2. Field surveys (dataset 4)

Because of the high concentrations of PST accumulated by oysters in the field (until 20 times more than the concentrations observed in the laboratory experiments), PST effects upon the energy budget led to an unrealistic decrease in the oyster flesh mass for the simulated individuals when using the $[PST]_q$ value estimated from dataset 1 (predicted mass close to zero, not shown). This problem was solved by fixing $[PST]_q$ to 50 µg STX eq. $100g^{-1}$.

During the 2012 field survey, the concentrations of *A. minutum* cells in seawater at Pointe-du-Chateau were found to range between $1.7\ 10^3$ and $8\ 10^6$ cell L^{-1}. The value of the parameter ρ_{PST} was adjusted to 0.086 µg STX eq. J^{-1} to enable an accurate model prediction of the PST accumulation in oyster tissues (Fig. 7).

In 2013, the *A. minutum* bloom was less intense (highest concentration reached $3\ 10^5$ cell L^{-1}) and was associated with a low accumulation of PST by oysters (Fig. 8). During this survey, oysters were kept in the field until the *A. minutum* bloom collapsed. The cellular concentration ranged from 1.4 to 9.0 pg STX-diHCl eq. $cell^{-1}$ during the monitoring period. For parsimony purposes, model predictions were performed with a constant ρ_{PST} value (0.463 µg STX eq. J^{-1}), which enabled us to properly reproduce the observed dynamics of PST during the monitoring (Fig. 8).

In 2014, the cell counts of *A. minutum* measured in the field ranged between $5\ 10^3$ and 10^6 cell L^{-1}. The parameter ρ_{PST} was adjusted to a value of 0.431 µg STX eq. J^{-1}. Using temperature and algal concentrations (non-toxic and toxic) as forcing variables allowed the model to predict the observed dynamics of toxin accumulation in oyster tissues (Fig. 9). Finally, the inter-individual variability was lower in the field surveys than in the laboratory experiments. Indeed, individuals with an intermediate accumulation potential

(continuous grey lines) associated to different initial masses were sufficient to describe the variability in PST accumulation observed in the three field surveys.

4. Discussion

4.1. Relationship between A. minutum cell density during exposure and PST accumulation

During the three years of field monitoring, accumulation of PST was observed in oysters with a maximum concentration of 40 $\mu g\,STX\,eq.\,100g^{-1}$ in 2013 and of 300 $\mu g\,STX\,eq.\,100g^{-1}$ in 2012 after exposure to *A. minutum* at cell densities between $3\,10^5$ and $8\,10^6$ $cell\,L^{-1}$. During the experiment conducted by Pousse et al. (2017) (dataset 2), with *A. minutum* only, the maximum concentration in oysters reached 173 $\mu g\,STX\,eq.\,100g^{-1}$ after oysters were exposed to $1.8\,10^6$ $cell\,L^{-1}$ of *A. minutum*. In contrast, accumulation values in both datasets 1 and 3 were surprisingly low (close to 10 $\mu g\,STX\,eq.\,100g^{-1}$) ; whereas, the cell density of *A. minutum* during exposure was close to those observed in the field. During these two experiments, oysters were exposed to both toxic and non-toxic algae, conversely oysters were only or mainly exposed to *A. minutum* in Pousse et al. (2017) or during the *A. minutum* blooms 2012-2014.

The low accumulation observed when oysters were fed with both toxic and non-toxic algae may be explained by particle selection. The pre-ingestive selection is a well-known phenomenon in bivalves based upon complex mechanisms. It is unlikely that selection relies upon the presence of toxins (internal), but might rather be attributable to an external signature (carbohydrate; signature, Espinosa et al., 2016) or to surface physical properties of the algal cell (wetability, charge; Rosa et al., 2017b). Although probably not based upon cellular toxicity, it has been shown that particle selection allows low toxin intake when toxic algae are present in high concentration mixed with non-toxic algae (Mafra et al., 2009). In contrast, when only *A. minutum* is present in the water column, which is the case during intense blooms, it is used as the main food source by oysters.

We used synthesizing units (Kooijman, 1998) to deal with these selection processes as already applied in bivalves (Kooijman, 2006; Saraiva et al., 2011; Lavaud et al., 2014). To our knowledge, it is the first time that SUs were implemented to describe toxicant intake. The SU scheme used has been described by Kooijman (2010) and used in Lavaud et al. (2014); it allows one to deal with substitutable substrates that bind sequentially and to replace one substrate with another. The present study showed that this formulation was effective in understanding oyster food preference when exposed to *A. minutum* and non-toxic algae.

4.2. Toxin dynamics

Some modelling studies modelled PST dynamics with a single compartment (Blanco et al., 1997; Chen and Chou, 2001; Blanco et al., 2003; Guéguen et al., 2011). Nevertheless, most authors agreed on the fact that two elimination pathways (metabolization and egestion) were needed. Because these two pathways imply different location of toxins accumulation with different temporal dynamics, we intuitively developed our model with two compartments of accumulation. This model can also be expressed with a single compartment, however, the parameters gain is null and complicate the study of the two toxin elimination pathways. Moreover, if we imagine an application of this model to other bivalves in which the digestive gland is generally not consumed by humans (most Pectinidae), our approach based upon two compartments would be useful. The unassimilated toxins compartment would remain identical while the assimilated toxins compartment would be composed of sub-compartments corresponding to each organ of interest. Transfers between organs and their specific elimination rate are the parameters to be added.

As developed in Silvert and Cembella (1995) or Lassus et al. (2007), toxin dynamics were modelled through two-compartments: unassimilated toxins (digestive tract content in toxins, Q_U) and internal toxin content (assimilated toxins, Q_A). Because gut transit time is short (Guéguen et al., 2008b), introducing the unassimilated toxins compartment into the model was thought to account for the fast-dynamics of the digestive tract. Nevertheless, our estimation indicated that this compartment could account for up to 50 % of the total amount of toxins (data not shown). For parsimony purposes, the gut transit time was only considered to be dependent on oyster length and temperature, but this dynamic could be improved by taking into account a dependence on feeding rate (Navarro et al., 1992; Moroño et al., 2001). Our work also showed that a first order process efficiently described elimination of assimilated toxins. We estimated the elimination constant to 0.17 d^{-1} which is similar to values found for other models on bivalves (0.31, 0.22, and 0.28 in average for *C. gigas*, Yamamoto et al., 2003; Lassus et al., 2007; Guéguen et al., 2011, respectively; 0.17 and 0.15 for mussels, Hurst and Gilfillan, 1977; Blanco et al., 2003; 0.1 and 0.09 for clams, Hurst and Gilfillan, 1977; Chen and Chou, 2001; 0.1 for quahog, Bricelj et al., 1991). This value has been estimated with the detoxification data where oysters were starved (in filtrated seawater). However, different studies have shown that oysters feeding on non-toxic algae after an exposure to toxic algae could reduce their detoxification time (Lassus et al., 2000, 2005; Guéguen et al., 2008a). Bricelj and Shumway (1998) suggested that it was linked to an increase in the gut evacuation rate and to metabolism acceleration. According to these results, it would be worthwhile to run a detoxification experiment and compare oysters fed on non-toxic algae with starved

oysters to quantify the effect of oyster feeding during detoxification phase and determine whether it should be integrated into the model.

A few model underestimations can be observed on the results of 2013 and 2014 field surveys (Fig. 8 and 9 respectively) while PST concentrations were measured in the digestive gland. These ones appear mainly at the beginning of accumulation stages (days 6 and 10 in Fig. 8 ; day 21 in Fig. 9). Actually, these observations of PST concentrations are likely overestimated during accumulation stages since these measurements were made on oyster digestive glands. We converted PST concentrations measured in digestive gland into concentration in the whole flesh by assuming that 80% of the PST are localized in the digestive gland (Guéguen, 2009). In reality, it is probably not the case at the beginning of intoxication stage, since toxins should be almost entirely localized in the digestive gland, which gathers unassimilated toxins and assimilated toxins that are not transferred to other tissues yet. Note that the model parameters have been fully estimated on PST concentrations measured in whole flesh data thus model predictions were not altered by this measurement bias.

This model has been calibrated and validated on measurements of PST concentrations mostly obtained by ELISA. This measurement technique is known to be less accurate than HPLC methods, especially when biotransformations occur. The ELISA bioassay is manufactured to detect 100% of the saxitoxin quantity present in a sample. In contrast, others PSP toxins are not fully recognized, so that PST concentrations measurements may be sometimes underestimated with this technique (Dorantes-Aranda et al., 2017) as a result of cross-reactivity of each PST analogue. This reason could potentially explain why PST measurements are particularly low at days 7 and 21 in Fig. 3. To study the measurement deviations between PST concentrations obtained by ELISA and HPLC, some samples belonging to the dataset 4 were treated simultaneously with these two techniques. Results show that measurements were strongly and linearly correlated (r^2=0.91), and that ELISA tends to slightly overestimate the PST concentration with a factor equal to 1.04 (Appendix 4.2, Fig. S3).To take into account more accurately observations obtained from ELISA assays, one alternative could be to integrate the different biotransformations occurring in oysters in the model, as it was developed in some other models (Chen and Chou, 2001; Blanco et al., 2003). To calibrate this model, PSP toxin profiles in oysters as well as data on the variables that influence biotransformation would be needed.

4.3. ρ_{PST} parameter

In our model, the parameter ρ_{PST} accounts for the quantity of toxins per algal energy content; if the energy per *A. minutum* cell remains constant, this value might directly relate to the cellular PST content. As shown above, this value had to be adjusted to fit the model on each data set. The estimated ρ_{PST} values ranged from 0.086 to 0.463 $\mu g\,STX\,eq.\,J^{-1}$, with a factor 5.3 between the lowest and the highest values. The PST content of *A. minutum* is known to be highly variable, and differences in toxicity with a factor of 6.5 have been reported for a single *A. minutum* strain (Béchemin et al., 1999). The range of variation in ρ_{PST} parameter values in our study thus seems to be consistent with general knowledge. Variations in *A. minutum* PST cellular content might change with strain or growth conditions (Boyer et al., 1987; Anderson et al., 1990; Hwang and Lu, 2000). In addition, algal energy content has also been observed to be linked to environmental conditions (Renaud et al., 2002). As both parameters affect ρ_{PST} value, the fact that we adjusted different values is not surprising.

PST cellular content of *A. minutum* cells during the bloom monitored in 2013 ranged from 1.4 to 9.0 pg STX-diHCl eq. $cell^{-1}$ within a short time scale. Although the model was run with a constant value for ρ_{PST} ($0.463\ \mu g\,STX\,eq.\,J^{-1}$), it allowed a satisfying fit between model and observations. The model seems thus robust to predict toxin accumulation on short time scales.

The PST cellular content of the *A. minutum* strain used in datasets 1 and 2 was 24.5 times lower than that used in dataset 3 (0.053 against 1.3 pg STX-diHCl eq. $cell^{-1}$). We estimated ρ_{PST} values of 0.13 and $0.15\ \mu g\,STX\,eq.\,J^{-1}$, corresponding to a factor of 1.15. Such a difference in the factor might be attributable either to different energy content per cell (which is unlikely because culture conditions were identical) or to the fact that the latter strain produces some other toxic compounds than PST. It has been shown that some *Alexandrium* spp. strains are able to produce extracellular toxic compounds (Arzul et al., 1999) known to have allelopathic activity on algae (Ma et al., 2011; Lelong et al., 2011) and ichtyotoxic activity on bivalves (Ford et al., 2008; Borcier et al., 2017; Castrec et al., 2018). Recent studies using the AM89BM *A. minutum* strain (used in the dataset 3) suggested that these compounds might also negatively affect feeding behavior in *Pecten maximus* (Borcier et al., 2017) and *C. gigas* (Castrec et al., 2018). Such differences in the feeding behavior of *C. gigas* might explain the relatively low value estimated for ρ_{PST} in dataset 3. In other words, it is likely that extracellular compounds caused oysters to ingest fewer *A. minutum* cells than expected by the model, thus resulting in an underestimation of the ρ_{PST} value.

To improve model prediction of accumulation, further work is needed to better describe the relationship

between ρ_{PST} value and PST cellular content. Moreover, measuring PST cellular content and also estimating the quantity of extracellular compounds or their toxicity, in addition to *A. minutum* environmental concentration during field monitoring, would provide better data to understand the relationship between *A. minutum* blooms and PST accumulation in oysters. For a management purpose where a specific sanitary threshold is set, we also recommend to adjust the ρ_{PST} parameter on observed data measured by official HPLC methods for PST quantification for more precise predictions.

4.4. Links between oysters energy budget and PST dynamics in oyster tissues

Coupling an oyster DEB model and PST accumulation model allows one to account for the effects of size and energetic status upon toxin accumulation and detoxification processes. As discussed previously, the unique accumulation pathway is through feeding. Processes involved in feeding (filtration activity and ingestion) are proportional to structural surface area (Kooijman, 2010). However, ingested toxins are diluted in the total volume/mass of the animal (structure, reserves and gonad). Thus with an identical exposure to toxic algae, small individuals are expected to accumulate higher concentrations of toxins than larger individuals. Such a pattern has been observed in Aalvik and Framstad (1981) and discussed in the review of Bricelj and Shumway (1998). This pattern might sometimes be hidden in experimental data as, for a given structural size, oysters with the highest reserve quantity will accumulate less than others as PST are diluted in an higher biovolume. The DEB-PST model allows one to predict these trends which strengthens the interest of coupling accumulation and bioenergetic models.

Effects of PST upon bivalves physiology have been widely documented. PST are known to affect hemocytes, gills, or muscles (Haberkorn et al., 2010a,b) and trigger defence or immune response. However, only a few studies quantified the consequences of exposure to PST on bivalve energy budget. Li et al. (2002) observed a decrease in the scope for growth, even at low PST concentrations (2.6 and 5.22 μg STX eq. $100g^{-1}$ respectively for *Ruditapes philippinarum* and *Perna viridis*), thus supporting our choice to integrate the effects of PST and with a low no-effect concentration (i.e. $[PST]_{NEC}$=0.1 μg STX eq. $100g^{-1}$). Different studies reported declines in bivalve growth rates during an exposure to PST-producing algae (Erard-Le Denn et al., 1990; Nielsen and Strømgren, 1991; Bricelj et al., 1993; Luckenbach et al., 1993). Based upon these observations, we assumed that PST affected maintenance costs and calibrated these effects with growth experiments. Although uncertainty remains concerning the quantification of these effects ($[PST]_q$ estimated in the laboratory experiment were not applicable in the field) we suggest that these effects are not negligible

because we estimated that maintenance costs were increased by a factor 1.5 in dataset 3 (Fig. 5). Such a value has to be confirmed by laboratory experiments in which higher PST concentration would be reached.

The formulation for PST effect upon maintenance cost does not take into account potential time-lagged effects on the energy budget (i.e. once toxins are eliminated, no effects remain on maintenance costs). Nevertheless, results presented in figure 5 (B) tend to indicate that PST-induced effects upon energy balance last longer than contamination as shrinking is still underestimated by the model when oysters have completely depurated. Such effects might be related to energy needed for tissue damage repair that may last longer than PST elimination.

Effects were applied to maintenance costs in this model, however, PST can also alter reproductive functions such as gamete viability (Haberkorn et al., 2010a). From data presented in the literature, an accurate calibration of these effects appears difficult and would benefit from a dedicated experiment, where number and energetic content of oocytes in individuals with varying PST burden would be measured. Furthermore, extending this model to all oyster life stages does not seem to be warranted, as Yan et al. (2001) shed light on the fact that decreases in egg hatching and larval survival during exposure to *Alexandrium tamarense* could be associated with extracellular compounds rather than PST.

Parameter $[PST]_q$ (toxicant stress concentration) estimated from dataset 1 was, unfortunately, not validated with the second laboratory experiment (dataset 3) nor with field data (dataset 4). Two different reasons could potentially explain this. In dataset 3, effects were underestimated. It is likely that the extracellular compounds synthesized by the *A. minutum* strain used in this validation laboratory experiment are responsible for these effects by means of (1) an increase in oyster tissues alteration (Ford et al., 2008) and (2) a decrease in oyster feeding (Borcier et al., 2017; Castrec et al., 2018). It would be worthwhile investigating bioenergetic costs caused by extracellular compounds to validate these two hypotheses. PST effects were conversely overestimated for the field surveys as the model initially predicted a lethal mass loss in oysters according to the environmental parameters. Three hypotheses could explain this phenomenon. (1) Either PST induced less effects upon oysters held in the field, (2) oysters held in the field were less sensitive to toxins or (3) *A. minutum* synthesizes less extracellular compounds in the field or have lesser effects upon oyster bioenergetics. Oysters placed in the field and exposed in laboratory had different life experiences. Before being transferred in the study site, field oysters spent time in natural environment, where they could have been in contact with toxic algae. The effects of a prior exposure to toxic algae have already been observed to cause higher feeding rates and PST loads in bivalves previously exposed (Shumway and Cucci,

1987; Chebib et al., 1993; Bricelj and Shumway, 1998). Moreover a recent study observed that in *C. gigas*, the nerves, which are the main STX targets, were less sensitive if the oysters had previously been exposed to toxic algae (Boullot et al., 2018). Taking these results into account, it can be hypothesized that a prior exposure to toxic algae may allow oysters to acquire a resistance to PST, i.e. exposures following the first contact with toxic algae have smaller effects on *C. gigas* maintenance costs. Field PST-induced effects or quantity of extracellular compounds synthesized by *A. minutum* in the environment should be further studied by comparing PST and extracellular compounds effects on *C. gigas* within laboratory or field conditions.

5. Conclusion

Results presented in this study showed that linking bioaccumulation processes to energy balance, by coupling bioaccumulation processes to a bioenergetic model based upon DEB theory allowed to properly predict PST accumulation and to deal with weight loss associated to PST effects. Based upon partitioning of the whole toxin quantity into two compartments (unassimilated and assimilated toxins), this model accurately describes accumulation kinetics of PST in *C. gigas* by taking into account individual oyster condition and environmental variables. Furthermore, the fact that this model calibrated with laboratory experiments can be applied in the field, where trophic and environmental conditions are relatively different, contributes to demonstrate its robustness. However, a difficulty remains concerning the STX amount per energy units in a toxic algae (ρ_{PST}) which needs to be adjusted according to the toxicity of the *A. minutum* strain known to be variable. This is the first time that the effects of PST were treated in a growth model and validated under laboratory conditions. Results also show that quantifying the effects of PST upon oyster bioenergetics is difficult and had to be adjusted according to the *A. minutum* strain and the exposure conditions (i.e. laboratory or field) to fit with observations. It is unlikely that the PST effects upon oysters are highly variable from strain to strain, we rather hypothesize that extracellular compounds synthesized by *A. minutum* in addition to PST, that are variable from strain to strain, might contribute to the effects of *A. minutum* upon the oyster energy balance. This model offers a new tool for the study and the monitoring of PST accumulation. Further studies should test different scenarios where biological functions such as gametogenesis, or the ploidy or mass would be modified to identify risky conditions leading to high PST loads in oysters.

6. Acknowledgements

We are warmly grateful to Bruno Petton at the Ifremer experimental facilities in Argenton for providing SPF oysters, and Jacqueline Le Grand and Dominique Ratiskol for producing the non-toxic algae. We also thank Matthias Huber, Isabelle Quéau, Christian Mingant, Marion Riobé, Valérian Le Roy, Loann Gissat and Mélaine Gourault, for their technical help. We thank Élodie Fleury for providing oysters placed in the field and Gary H. Wikfors for assistance with english editing and relevant comments. Field data (algal concentrations, PST contents in algae and oysters) were measured within the framework of the project "DAOULEX". Seawater temperature data from the Bay of Brest were provided by SOMLIT network. Algae enumerations were realized by A. Piraud from "AEL plancton".

This study was carried out with the financial support of the French National Research Agency (ANR) “ACCUTOX” project (ANR-13-CESA-0019 2013–2017). This work is part of a PhD project supported by the "Laboratoire d’Exellence" LabexMer (ANR-10-LABX-19) and co-founded by a grant from the French government under the program "Investissement d’Avenir", and by a grant of the Regional Council of Brittany.

7. References

Aalvik, B., Framstad, K., 1981. Assay and detoxification experiments with Mytilotoxin in mussels (*Mythus edulis* L.) from Nordåsstraumen, Western Norway, 1979 and 1980. Sarsia 66 (2), 143–146.

Alunno-Bruscia, M., Bourlès, Y., Maurer, D., Robert, S., Mazurié, J., Gangnery, A., Goulletquer, P., Pouvreau, S., 2011. A single bio-energetics growth and reproduction model for the oyster *Crassostrea gigas* in six Atlantic ecosystems. J. Sea Res. 66 (4), 340–348.

Anderson, D., Kulis, D., Sullivan, J., Hall, S., 1990. Toxin composition variations in one isolate of the dinoflagellate *Alexandrium fundyense*. Toxicon 28 (8), 885–893.

Anderson, D. M., 1989. Toxic algal blooms and red tides : a global perspective. Red tides : Biology, environmental science and toxicology, 11–16.

Anderson, D. M., Glibert, P. M., Burkholder, J. M., 2002. Harmful algal blooms and eutrophication : nutrient sources, composition, and consequences. Estuaries 25 (4), 704–726.

Arzul, G., Seguel, M., Guzman, L., Erard-Le Denn, E., 1999. Comparison of allelopathic properties in three toxic *Alexandrium* species. J. Exp. Mar. Biol. Ecol. 232 (2), 285–295.

Barillé, L., Prou, J., Héral, M., Bourgrier, S., 1993. No influence of food quality, but ration-dependent retention efficiencies in the Japanese oyster *Crassostrea gigas*. J. Exp. Mar. Biol. Ecol. 171 (1), 91–106.

Béchemin, C., Grzebyk, D., Hachame, F., Hummert, C., Maestrini, S. Y., 1999. Effect of different nitrogen/phosphorus nutrient ratios on the toxin content in *Alexandrium minutum*. Aquat. Microb. Ecol. 20 (2), 157–165.

Bernard, I., De Kermoysan, G., Pouvreau, S., 2011. Effect of phytoplankton and temperature on the reproduction of the Pacific oyster *Crassostrea gigas* : investigation through DEB theory. J. Sea Res. 66 (4), 349–360.

Blanco, J., Moroño, A., Franco, J., Reyero, M., 1997. PSP detoxification kinetics in the mussel *Mytilus galloprovincialis*. one-and two-compartment models and the effect of some environmental variables. Mar. Ecol. Prog. Ser., 165–175.

Blanco, J., Reyero, M. I., Franco, J., 2003. Kinetics of accumulation and transformation of paralytic shellfish toxins in the blue mussel *Mytilus galloprovincialis*. Toxicon 42 (7), 777–784.

Bodiguel, X., Maury, O., Mellon-Duval, C., Roupsard, F., Le Guellec, A.-M., Loizeau, V., 2009. A dynamic and mechanistic model of PCB bioaccumulation in the European hake (*Merluccius merluccius*). J. Sea Res. 62 (2), 124–134.

Borcier, E., Morvezen, R., Boudry, P., Miner, P., Charrier, G., Laroche, J., Hegaret, H., 2017. Effects of bioactive extracellular compounds and paralytic shellfish toxins produced by *Alexandrium minutum* on growth and behaviour of juvenile great scallops *Pecten maximus*. Aquat. Toxicol..

Bougrier, S., Geairon, P., Deslous-Paoli, J., Bacher, C., Jonquières, G., 1995. Allometric relationships and effects of temperature on clearance and oxygen consumption rates of *Crassostrea gigas* (Thunberg). Aquaculture 134 (1), 143–154.

Boullot, F., Fabioux, C., Hegaret, H., Soudant, P., Boudry, P., Benoit, E., 2018. Assessment of saxitoxin sensitivity of nerves isolated from the Pacific oyster, *Crassostrea gigas*, exposed to *Alexandrium minutum*. Toxicon 149, 93.

Bourlès, Y., Alunno-Bruscia, M., Pouvreau, S., Tollu, G., Leguay, D., Arnaud, C., Goulletquer, P., Kooijman, S., 2009. Modelling growth and reproduction of the Pacific oyster *Crassostrea gigas* : advances in the oyster-DEB model through application to a coastal pond. J. Sea Res. 62 (2), 62–71.

Boyer, G., Sullivan, J., Andersen, R., Harrison, P., Taylor, F., 1987. Effects of nutrient limitation on toxin production and composition in the marine dinoflagellate *Protogonyaulax tamarensis*. Mar. Biol. 96 (1), 123–128.

Bricelj, V., Greene, M., Lee, J., Cembella, A., 1993. Growth of the blue mussel *Mytilus edulis* on toxic *Alexandrium fundyense* and effects of gut passage on dinoflagellate cells. In : Toxic Phytoplankton Blooms in the Sea. Elsevier, Amsterdam, TJ Smayda, Y. Shimuzu (Eds.), pp. 371–376.

Bricelj, V., Lee, J., Cembella, A., 1991. Influence of dinoflagellate cell toxicity on uptake and loss of paralytic shellfish toxins in the northern quahog *Mercenaria mercenaria*. Mar. Ecol. Prog. Ser. 74, 33–46.

Bricelj, V., Lee, J., Cembella, A., Anderson, D., 1990. Uptake kinetics of paralytic shellfish toxins from the dinoflagellate *Alexandrium fundyense* in the mussel *Mytilus edulis*. Mar. Ecol. Prog. Ser. 63 (2), 177–188.

Bricelj, V. M., Shumway, S. E., 1998. Paralytic shellfish toxins in bivalve molluscs : occurrence, transfer kinetics, and biotransformation. Rev. Fish. Sci. 6 (4), 315–383.

Casas, S., Bacher, C., 2006. Modelling trace metal (Hg and Pb) bioaccumulation in the mediterranean mussel, *Mytilus galloprovincialis*, applied to environmental monitoring. J. Sea Res. 56 (2), 168–181.

Castrec, J., Soudant, P., Payton, L., Tran, D., Miner, P., Lambert, C., Le Goïc, N., Huvet, A., Quillien, V., Boullot, F., Amzil, Z., Hégaret, H., Fabioux, C., 2018. Bioactive extracellular compounds produced by the dinoflagellate *Alexandrium minutum* are highly detrimental for oysters. Aquat. Toxicol..

Cembella, A., 1998. Ecophysiology and metabolism of paralytic shellfish toxins in marine microalgae. In : Physiological Ecology of Harmful Algal Blooms, Heidelberg, Anderson, DM, AD Cembella, GM Hallegraeff (Eds.), NATO-Advanced Study Institute Series. Vol. 41. Springer-Verlag, pp. 381–404.

Cembella, A. D., Shumway, S. E., Larocque, R., 1994. Sequestering and putative biotransformation of paralytic shellfish toxins by the sea scallop *Placopecten magellanicus* : seasonal and spatial scales in natural populations. J. Exp. Mar. Biol. Ecol. 180 (1), 1–22.

Chapelle, A., Le Gac, M., Labry, C., Siano, R., Quere, J., Caradec, F., Le Bec, C., Nezan, E., Doner, A., Gouriou, J., 2015. The Bay of Brest (France), a new risky site for toxic *Alexandrium minutum* blooms and PSP shellfish contamination. Harmful Algae News 51, 4–5.

Chebib, H., Cembella, A., Anderson, P., 1993. Differential paralytic shellfish toxin accumulation and detoxification kinetics in transplanted populations of *Mytilus edulis* exposed to natural blooms of *Alexandrium excavatum*. DEV. MAR. BIOL.

Chen, C. Y., Chou, H. N., 2001. Accumulation and depuration of paralytic shellfish poisoning toxins by purple clam *Hiatula rostrata* Lighttoot. Toxicon 39 (7), 1029–1034.

Chou, H. N., Chen, Y. M., Chen, C. Y., 2004. Variety of PSP toxins in four culture strains of *Alexandrium minutum* collected from southern Taiwan. Toxicon 43 (3), 337–340.

Dorantes-Aranda, J. J., Campbell, K., Bradbury, A., Elliott, C. T., Harwood, D. T., Murray, S. A., Ugalde, S. C., Wilson, K., Burgoyne, M., Hallegraeff, G. M., 2017. Comparative performance of four immunological test kits for the detection of Paralytic Shellfish Toxins in Tasmanian shellfish. Toxicon 125, 110–119.

EFSA, 2009. Marine biotoxins in shellfish–saxitoxin group. EFSA journal 7 (4), 1019.

Eichinger, M., Loizeau, V., Roupsard, F., Le Guellec, A.-M., Bacher, C., 2010. Modelling growth and bioaccumulation of Polychlorinated biphenyls in common sole (*Solea solea*). J. Sea Res. 64 (3), 373–385.

Erard-Le Denn, E., Morlaix, M., Dao, J., 1990. Effects of *Gyrodinium* cf. *aureolum* on *Pecten maximus* (post larvae, juveniles and adults). In : Toxic Marine Phytoplankton. Elsevier, North Holland, pp. 132–136.

Espinosa, E. P., Cerrato, R. M., Wikfors, G. H., Allam, B., 2016. Modeling food choice in the two suspension-feeding bivalves, *Crassostrea virginica* and *Mytilus edulis*. Mar. Biol. 163 (2), 40.

Fabioux, C., Sulistiyani, Y., Haberkorn, H., Hégaret, H., Amzil, Z., Soudant, P., 2015. Exposure to toxic *Alexandrium minutum* activates the detoxifying and antioxidant systems in gills of the oyster *Crassostrea gigas*. Harmful Algae 48, 55–62.

Ford, S. E., Bricelj, V. M., Lambert, C., Paillard, C., 2008. Deleterious effects of a nonpst bioactive compound (s) from *Alexandrium tamarense* on bivalve hemocytes. Mar. Biol. 154 (2), 241–253.

Gourault, M., Petton, S., Thomas, Y., Pecquerie, L., Marques, G. M., Cassou, C., Fleury, E., Paulet, Y.-M., Pouvreau, S., 2018. Modeling reproductive traits of an invasive bivalve species under contrasting climate scenarios from 1960 to 2100. Journal of Sea Research.

Guallar, C., Bacher, C., Chapelle, A., 2017. Global and local factors driving the phenology of *Alexandrium minutum* (Halim) blooms and its toxicity. Harmful Algae 67, 44–60.

Guéguen, M., 2009. Modélisation de la détoxication de mollusques bivalves contenant des phycotoxines paralysantes ou diarrhéiques. Ph.D. thesis, Nantes.

Guéguen, M., Bardouil, M., Baron, R., Lassus, P., Truquet, P., Massardier, J., Amzil, Z., 2008a. Detoxification of Pacific oyster *Crassostrea gigas* fed on diets of *Skeletonema costatum* with and without silt, following PSP contamination by *Alexandrium minutum*. Aquat. Living Resour. 21 (1), 13–20.

Guéguen, M., Baron, R., Bardouil, M., Truquet, P., Haberkorn, H., Lassus, P., Barillé, L., Amzil, Z., 2011. Modelling of paralytic shellfish toxin biotransformations in the course of *Crassostrea gigas* detoxification kinetics. Ecol. Model. 222 (18), 3394–3402.

Guéguen, M., Lassus, P., Laabir, M., Bardouil, M., Baron, R., Séchet, V., Truquet, P., Amzil, Z., Barillé, L., 2008b. Gut passage times in two bivalve molluscs fed toxic microalgae :*Alexandrium minutum*, *A. catenella* and *Pseudo-nitzschia calliantha*. Aquat. Living Resour. 21 (1), 21–29.

Haberkorn, H., Lambert, C., Le Goïc, N., Guéguen, M., Moal, J., Palacios, E., Lassus, P., Soudant, P., 2010a. Effects of *Alexandrium minutum* exposure upon physiological and hematological variables of diploid and triploid oysters, *Crassostrea gigas*. Aquat. Toxicol. 97 (2), 96–108.

Haberkorn, H., Lambert, C., Le Goïc, N., Moal, J., Suquet, M., Guéguen, M., Sunila, I., Soudant, P., 2010b. Effects of *Alexandrium minutum* exposure on nutrition-related processes and reproductive output in oysters *Crassostrea gigas*. Harmful Algae 9 (5), 427–439.

Hallegraeff, G. M., 1993. A review of harmful algal blooms and their apparent global increase. Phycologia 32 (2), 79–99.

Hallegraeff, G. M., Anderson, D. M., Cembella, A. D., Enevoldsen, H. O., et al., 2003. Manual on harmful marine microalgae. Unesco.

Hégaret, H., Brokordt, K. B., Gaymer, C. F., Lohrmann, K. B., García, C., Varela, D., 2012. Effects of the toxic dinoflagellate *Alexandrium catenella* on histopathogical and escape responses of the Northern scallop *Argopecten purpuratus*. Harmful Algae 18, 74–83.

Hégaret, H., Shumway, S. E., Wikfors, G. H., Pate, S., Burkholder, J. M., 2008. Potential transport of harmful algae via relocation of bivalve molluscs. Mar. Ecol. Prog. Ser. 361, 169–179.

Honsell, G., Poletti, R., Pompei, M., Sidari, L., Milandri, A., Casadei, C., Viviani, R., 1996. *Alexandrium minutum* Halim and PSP contamination in the northern Adriatic Sea (Mediterranean sea). Harmful Toxic Algal Blooms, 77–80.

Hurst, J. W., Gilfillan, E. S., 1977. Paralytic shellfish poisoning in Maine. Department of Marine Resources.

Hwang, D. F., Lu, Y. H., 2000. Influence of environmental and nutritional factors on growth, toxicity, and toxin profile of dinoflagellate *Alexandrium minutum*. Toxicon 38 (11), 1491–1503.

Jager, T., Barsi, A., Hamda, N. T., Martin, B. T., Zimmer, E. I., Ducrot, V., 2014. Dynamic energy budgets in population ecotoxicology : Applications and outlook. Ecol. Model. 280, 140–147.

Jager, T., Zimmer, E. I., 2012. Simplified dynamic energy budget model for analysing ecotoxicity data. Ecol. Model. 225, 74–81.

Kooijman, S., 1998. The synthesizing unit as model for the stoichiometric fusion and branching of metabolic fluxes. Bioph. Chem. 73 (1), 179–188.

Kooijman, S., Bedaux, J., 1996. Analysis of toxicity tests on fish growth. Wat. Res. 30 (7), 1633–1644.

Kooijman, S., Metz, J., 1984. On the dynamics of chemically stressed populations : the deduction of population consequences from effects on individuals. Ecotoxicol. Environ. Saf. 8 (3), 254–274.

Kooijman, S. A., 2006. Pseudo-faeces production in bivalves. J. Sea Res. 56, 103–106.

Kooijman, S. A. L. M., 2000. Dynamic energy and mass budgets in biological systems. Cambridge university press.

Kooijman, S. A. L. M., 2010. Dynamic energy budget theory for metabolic organisation. Cambridge university press.

Kwong, R. W., Wang, W.-X., Lam, P. K., Peter, K., 2006. The uptake, distribution and elimination of paralytic shellfish toxins in mussels and fish exposed to toxic dinoflagellates. Aquat. Toxicol. 80 (1), 82–91.

Laabir, M., Amzil, Z., Lassus, P., Masseret, E., Tapilatu, Y., De Vargas, R., Grzebyk, D., 2007. Viability, growth and toxicity of *Alexandrium catenella* and *Alexandrium minutum* (Dinophyceae) following ingestion and gut passage in the oyster *Crassostrea gigas*. Aquat. Living Resour. 20 (1), 51–57.

Lassudrie, M., Soudant, P., Nicolas, J.-L., Fabioux, C., Lambert, C., Miner, P., Le Grand, J., Petton, B., Hégaret, H., 2015a. Interaction between toxic dinoflagellate *Alexandrium catenella* exposure and disease associated with herpesvirus OsHV-1μvar in Pacific oyster spat *Crassostrea gigas*. Harmful Algae 45, 53–61.

Lassudrie, M., Wikfors, G. H., Sunila, I., Alix, J. H., Dixon, M. S., Combot, D., Soudant, P., Fabioux, C., Hégaret, H., 2015b. Physiological and pathological changes in the eastern oyster *Crassostrea virginica* infested with the trematode *Bucephalus sp.* and exposed to the toxic dinoflagellate *Alexandrium fundyense*. J. Invertebr. Pathol. 126, 51–63.

Lassus, P., Amzil, Z., Baron, R., Séchet, V., Barillé, L., Abadie, E., Bardouil, M., Sibat, M., Truquet, P., Bérard, J.-B., 2007. Modelling the accumulation of PSP toxins in Thau lagoon oysters (*Crassostrea gigas*) from trials using mixed cultures of *Alexandrium catenella* and *Thalassiosira weissflogii*. Aquat. Living Resour. 20 (01), 59–67.

Lassus, P., Bardouil, M., Baron, R., Berard, J.-B., Masselin, P., Truquet, P., Pitrat, J., 2005. Improving detoxification efficiency of PSP-contaminated oysters (*Crassostrea gigas* Thunberg). Aquaculture Eur..

Lassus, P., Bardouil, M., Massselin, P., Naviner, M., Truquet, P., 2000. Comparative efficiencies of different non-toxic microalgal diets in detoxification of PSP-contaminated oysters (*Crassostrea gigas* Thunberg). J. Nat. Toxins 9 (1), 1–12.

Lassus, P., Baron, R., Garen, P., Truquet, P., Masselin, P., Bardouil, M., Leguay, D., Amzil, Z., 2004. Paralytic shellfish poison outbreaks in the Penze estuary : Environmental factors affecting toxin uptake in the oyster, *Crassostrea gigas*. Aquat. Living Resour. 17 (2), 207–214.

Lavaud, R., Flye-Sainte-Marie, J., Jean, F., Emmery, A., Strand, Ø., Kooijman, S. A., 2014. Feeding and energetics of the great scallop, Pecten maximus, through a DEB model. J. Sea Res. 94, 5–18.

Lelong, A., Haberkorn, H., Le Goïc, N., Hégaret, H., Soudant, P., 2011. A new insight into allelopathic effects of *Alexandrium minutum* on photosynthesis and respiration of the diatom *Chaetoceros neogracile* revealed by photosynthetic-performance analysis and flow cytometry. Microb. Ecol. 62 (4), 919–930.

Leong, S. C. Y., Murata, A., Nagashima, Y., Taguchi, S., 2004. Variability in toxicity of the dinoflagellate*Alexandrium tamarense* in response to different nitrogen sources and concentrations. Toxicon 43 (4), 407–415.

Li, S.-C., Wang, W.-X., 2001. Radiotracer studies on the feeding of two marine bivalves on the toxic and nontoxic dinoflagellate *Alexandrium tamarense*. J. Exp. Mar. Biol. Ecol. 263 (1), 65–75.

Li, S.-C., Wang, W.-X., Hsieh, D. P., 2002. Effects of toxic dinoflagellate *Alexandrium tamarense* on the energy budgets and growth of two marine bivalves. Mar. Environ. Res. 53 (2), 145–160.

Long, M., Tallec, K., Soudant, P., Lambert, C., Le Grand, F., Sarthou, G., Jolley, D., Hégaret, H., 2018. A rapid quantitative fluorescence-based bioassay to study allelochemical interactions from *Alexandrium minutum*. Environ. Poll. .

Luckenbach, M., Sellner, K., Shumway, S., Greene, K., 1993. Effects of two bloom-forming dinoflagellates, *Prorocentrum minimum* and *Gyrodinium uncatenum*, on the growth and survival of the eastern oyster, *Crassostrea virginica* (Gmelin 1791). J. Shellfish Res. 12 (2), 411–415.

Ma, H., Krock, B., Tillmann, U., Muck, A., Wielsch, N., Svatoš, A., Cembella, A., 2011. Isolation of activity and partial characterization of large non-proteinaceous lytic allelochemicals produced by the marine dinoflagellate *Alexandrium tamarense*. Harmful Algae 11, 65–72.

Mafra, L. L., Bricelj, V. M., Ward, J. E., 2009. Mechanisms contributing to low domoic acid uptake by oysters feeding on *Pseudonitzschia* cells. II. Selective rejection. Aquat. Biol. 6, 213–226.

Moroño, A., Franco, J., Miranda, M., Reyero, M. I., Blanco, J., 2001. The effect of mussel size, temperature, seston volume, food quality and volume-specific toxin concentration on the uptake rate of PSP toxins by mussels (*Mytilus galloprovincialis* Lmk). J. Exp. Mar. Biol. Ecol. 257 (1), 117–132.

Navarro, E., Iglesias, J., Ortega, M., 1992. Natural sediment as a food source for the cockle *Cerastoderma edule* (L.) : effect of

variable particle concentration on feeding, digestion and the scope for growth. J. Exp. Mar. Biol. Ecol. 156 (1), 69–87.

Navarro, J. M., Contreras, A. M., 2010. An integrative response by *Mytilus chilensis* to the toxic dinoflagellate *Alexandrium catenella*. Mar. Biol. 157 (9), 1967–1974.

Nielsen, M., Strømgren, T., 1991. Shell growth response of mussels (*Mytilus edulis*) exposed to toxic microalgae. Mar. Biol. 108 (2), 263–267.

Oshima, Y., 1995. Chemical and enzymatic transformation of paralytic shellfish toxins in marine organisms. Harmful Marine Algal Blooms., 475–480.

Petton, B., Pernet, F., Robert, R., Boudry, P., 2013. Temperature influence on pathogen transmission and subsequent mortalities in juvenile Pacific oysters *Crassostrea gigas*. Aquac. Environ. Inter. 3, 257–273.

Pousse, É., Flye-Sainte-Marie, J., Alunno-Bruscia, M., Hégaret, H., Jean, F., 2017. Sources of paralytic shellfish toxin accumulation variability in the pacific oyster crassostrea gigas. Toxicon.

Pouvreau, S., Bourles, Y., Lefebvre, S., Gangnery, A., Alunno-Bruscia, M., 2006. Application of a dynamic energy budget model to the Pacific oyster, *Crassostrea gigas*, reared under various environmental conditions. J. Sea Res. 56 (2), 156–167.

Renaud, S. M., Thinh, L.-V., Lambrinidis, G., Parry, D. L., 2002. Effect of temperature on growth, chemical composition and fatty acid composition of tropical Australian microalgae grown in batch cultures. Aquaculture 211 (1), 195–214.

Reynolds, C. S., 2006. The ecology of phytoplankton. Cambridge University Press.

Rolland, J.-L., Medhioub, W., Vergnes, A., Abi-Khalil, C., Savar, V., Abadie, E., Masseret, E., Amzil, Z., Laabir, M., 2014. A feedback mechanism to control apoptosis occurs in the digestive gland of the oyster *Crassostrea gigas* exposed to the paralytic shellfish toxins producer *Alexandrium catenella*. Mar. Drugs 12 (9), 5035–5054.

Rosa, M., Ward, J. E., Frink, A., Shumway, S. E., 2017a. Effects of surface properties on particle capture by two species of suspension-feeding bivalve molluscs. Am. Malacol. Bull. 35 (2), 181–188.

Rosa, M., Ward, J. E., Holohan, B. A., Shumway, S. E., Wikfors, G. H., 2017b. Physicochemical surface properties of microalgae and their combined effects on particle selection by suspension-feeding bivalve molluscs. J. Exp. Mar. Biol. Ecol. 486, 59–68.

Rosa, M., Ward, J. E., Shumway, S. E., Wikfors, G. H., Pales-Espinosa, E., Allam, B., 2013. Effects of particle surface properties on feeding selectivity in the eastern oyster *Crassostrea virginica* and the blue mussel *Mytilus edulis*. J. Exp. Mar. Biol. Ecol. 446, 320–327.

Saraiva, S., Van Der Meer, J., Kooijman, S., Sousa, T., 2011. Modelling feeding processes in bivalves : a mechanistic approach. Ecol. Model. 222 (3), 514–523.

Shumway, S. E., 1990. A review of the effects of algal blooms on shellfish and aquaculture. J. World Aquac. Soc. 21 (2), 65–104.

Shumway, S. E., Cucci, T. L., 1987. The effects of the toxic dinoflagellate *Protogonyaulax tamarensis* on the feeding and behaviour of bivalve molluscs. Aquat. Toxicol. 10 (1), 9–27.

Silvert, W., Cembella, A., 1995. Dynamic modelling of phycotoxin kinetics in the blue mussel, *Mytilus edulis*, with implications for other marine invertebrates. Can. J. of Fish. Aquat. Sci. 52 (3), 521–531.

Soletchnik, P., Razet, D., Geairon, P., 1997. Ecophysiology of maturation and spawning in oyster (*Crassostrea gigas*) : metabolic (respiration) and feeding (clearance and absorption rates) responses at different maturation stages. Oceanogr. Lit. Rev. 12 (44), 1545.

Thomas, Y., Pouvreau, S., Alunno-Bruscia, M., Barillé, L., Gohin, F., Bryère, P., Gernez, P., 2016. Global change and climate-driven invasion of the Pacific oyster (*Crassostrea gigas*) along European coasts : a bioenergetics modelling approach. J. Biogeogr.

43 (3), 568–579.

Van Haren, R., Schepers, H., Kooijman, S., 1994. Dynamic energy budgets affect kinetics of xenobiotics in the marine mussel *Mytilus edulis*. Chemosphere 29 (2), 163–189.

Visciano, P., Schirone, M., Berti, M., Milandri, A., Tofalo, R., Suzzi, G., 2016. Marine biotoxins : occurrence, toxicity, regulatory limits and reference methods. Front. Microbiol. 7.

Ward, J., Levinton, J., Shumway, S., Cucci, T., 1998. Particle sorting in bivalves : *in vivo* determination of the pallial organs of selection. Mar. Biol. 131 (2), 283–292.

Ward, J. E., Shumway, S. E., 2004. Separating the grain from the chaff : particle selection in suspension-and deposit-feeding bivalves. J. Exp. Mar. Biol. Ecol. 300 (1), 83–130.

Yamamoto, T., Flynn, K. J., Takayama, H., 2003. Application of a two-compartment one-toxin model to predict the toxin accumulation in Pacific oysters in Hiroshima Bay, Japan. Fish. Sci. 69 (5), 944–950.

Yan, T., Zhou, M., Fu, M., Wang, Y., Yu, R., Li, J., 2001. Inhibition of egg hatching success and larvae survival of the scallop, *Chlamys farreri*, associated with exposure to cells and cell fragments of the dinoflagellate *Alexandrium tamarense*. Toxicon 39 (8), 1239–1244.

Yasumoto, T., Murata, M., 1993. Marine toxins. Chem. Rev. 93 (5), 1897–1909.

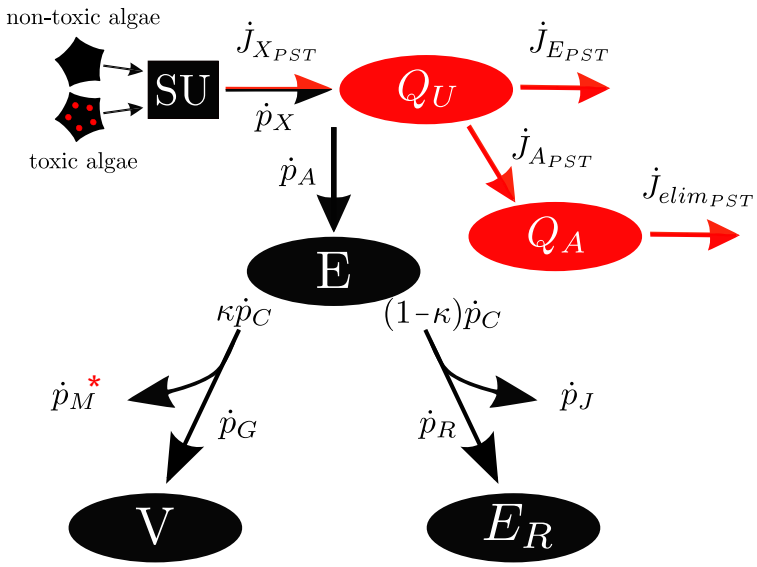

FIGURE 1: Schematic representation of the DEB-PST model. Arrows with their mathematical names illustrate energy (black) and PST (red) fluxes. Black and red ellipses correspond respectively to energy and PST compartments. The red asterisk shows the energetic flux affected by PST. The SU function implemented to take into account pre-ingestive sorting is figured by the black box.

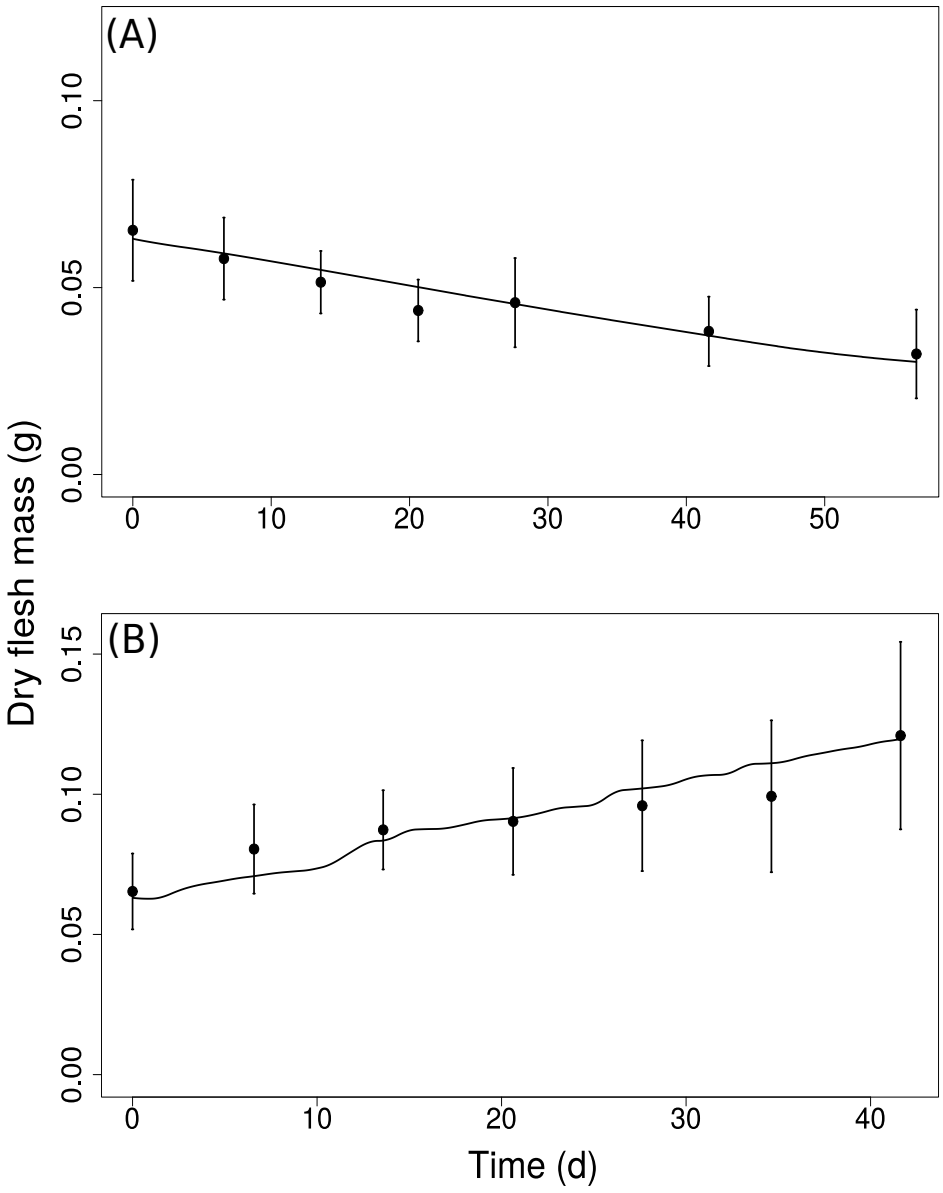

FIGURE 2: Observed (black dots, with vertical error bars as standard deviation) and DEB-predicted (lines) dry flesh mass of oysters over time in dataset 1, condition 1 (starvation for 8 weeks, A) and 2 (diet of non-toxic algae for 6 weeks, B). The black line is the average of simulations of 20 individuals.

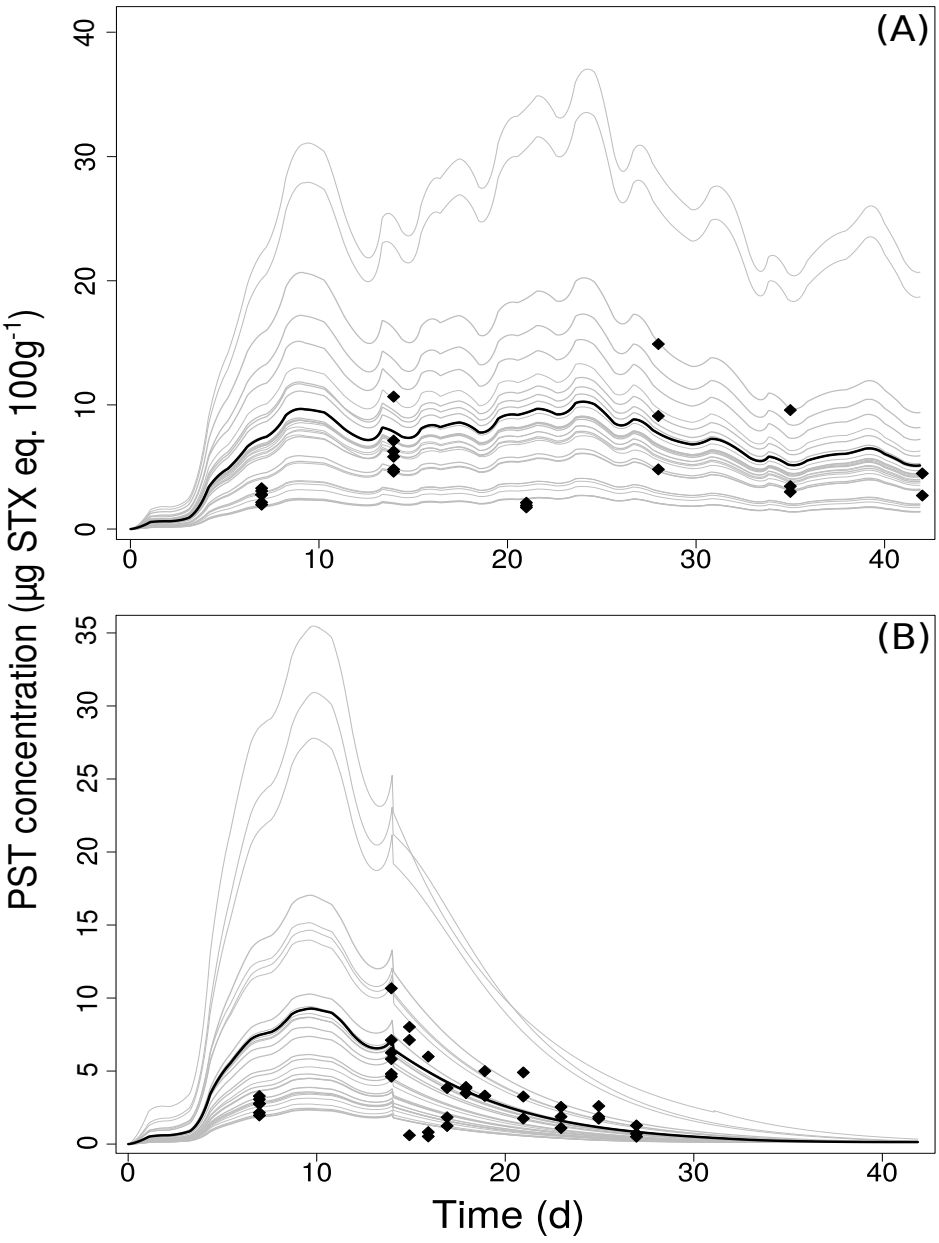

FIGURE 3: Observed (dots) and predicted (lines; grey: individual simulations of 20 individuals; black: average simulation) toxin concentrations in oyster tissues over time under condition 3 (A, a 6-week diet on both *A. minutum* and non-toxic algae) and condition 4 (B, a 2-week diet with both *A. minutum* and non-toxic algae, followed by 6 weeks in filtered seawater) of the dataset 1. In both conditions, the PST concentration was measured weekly on 15 individuals during exposure stages. In condition 4, PST content was measured daily on 3 individuals during the first 5 days of detoxification stage and every second day the following week. ρ_{PST} was adjusted to 0.130 µg STX eq. J^{-1}.

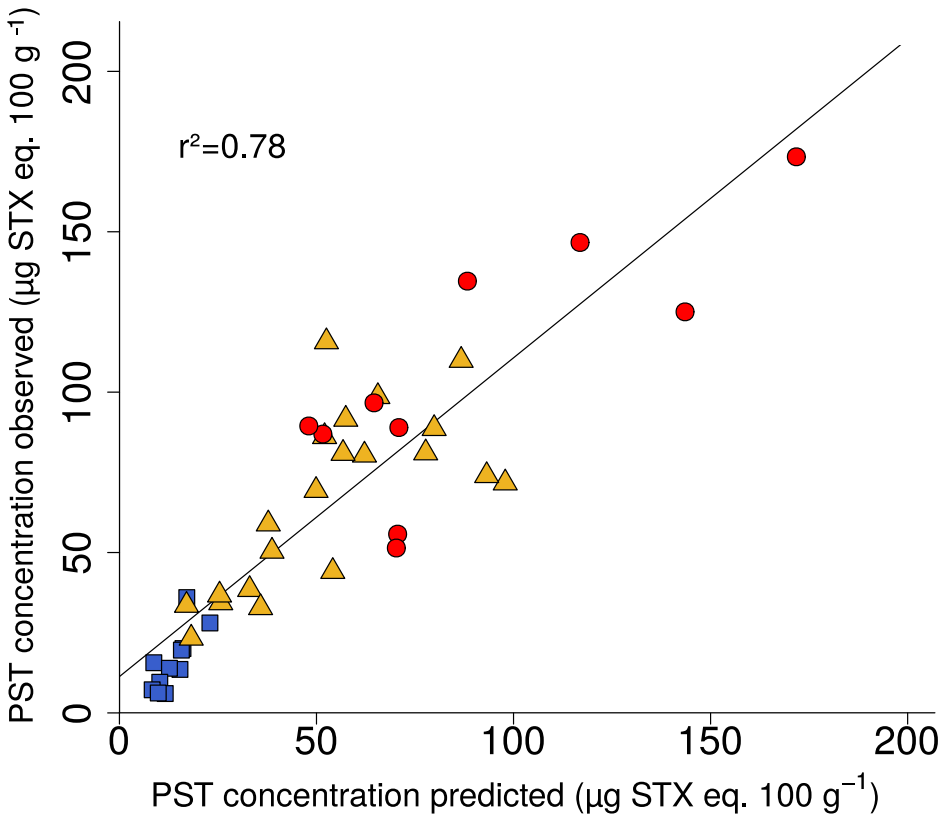

FIGURE 4: Observed versus predicted PST concentration in *C. gigas* (N=42) after 48-h exposure to *A. minutum* (see data from Pousse et al., 2017, dataset 2). Dots indicate the PST concentration measured in oyster tissues at 48 h. The three different potential of accumulation identified and attributed to each individual in Pousse et al. (2017) are represented by symbols and colours i.e. high accumulation (red circle), intermediate (yellow triangle), low (blue square). In the model, they correspond to different values for binding rates for toxic algae ($\{\dot{F}_{Tm}\}$; 1.5, 4, and 8 L d^{-1} cm^{-2}, respectively) measured in Pousse et al. (2017). The black line corresponds to the linear regression model adjusted on these data.

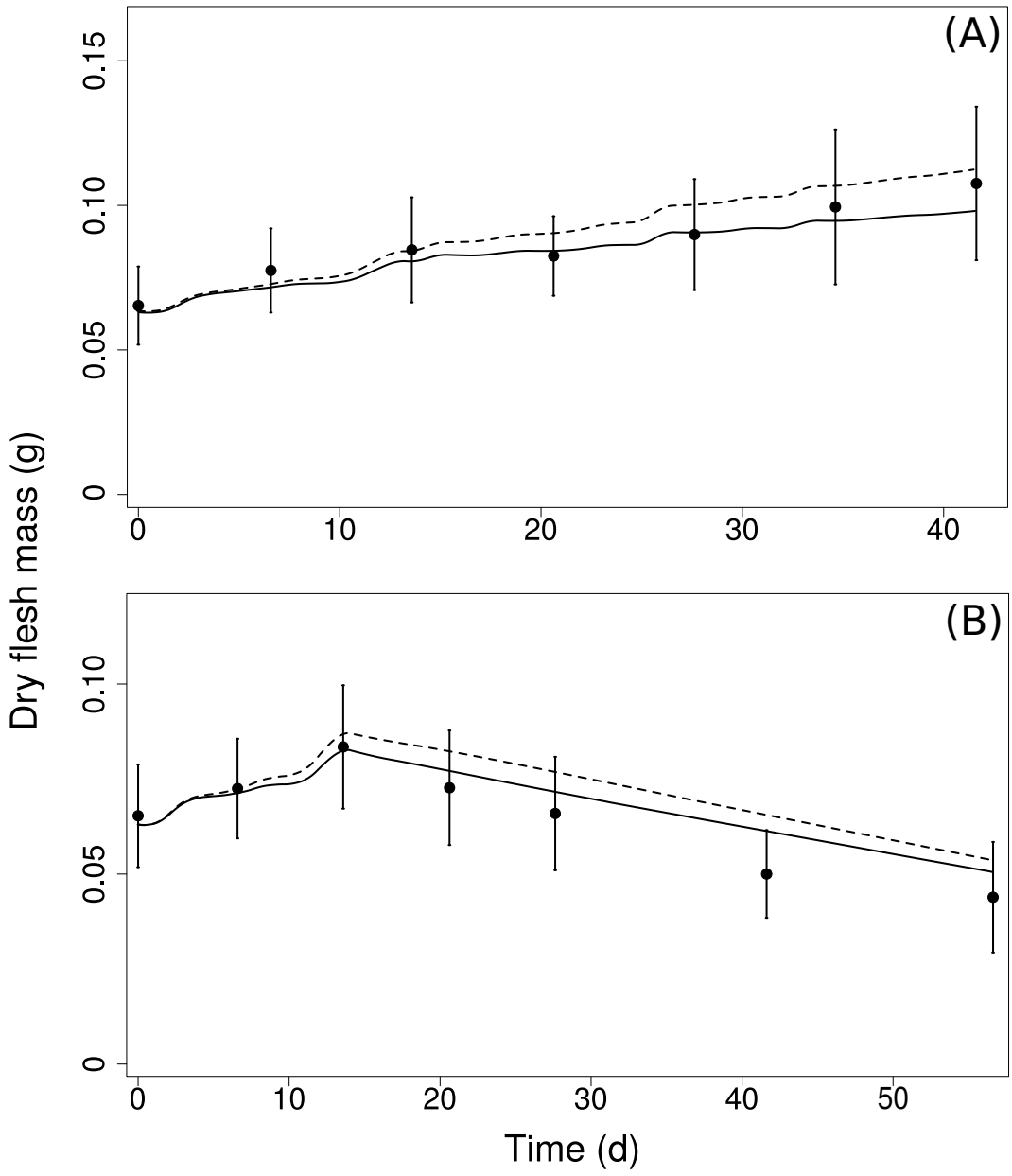

FIGURE 5: Observed (black dots, with vertical error bars as standard deviation) and predicted (lines) dry flesh mass (g) of oysters with and without PST effects on maintenance under condition 3 (A, 6-week diet with both *A. minutum* and non-toxic algae) and under condition 4 (B, 2-week diet with both *A. minutum* and non-toxic algae, followed by 6 weeks in filtered seawater) of dataset 1. Black continuous line indicates the mean of the trajectories of 20 individuals simulated including PST effect ($[PST]_q$ = 7 μgSTX eq. $100g^{-1}$), while black dashed line indicates the mean of the trajectories of 20 individuals simulated without PST effect.

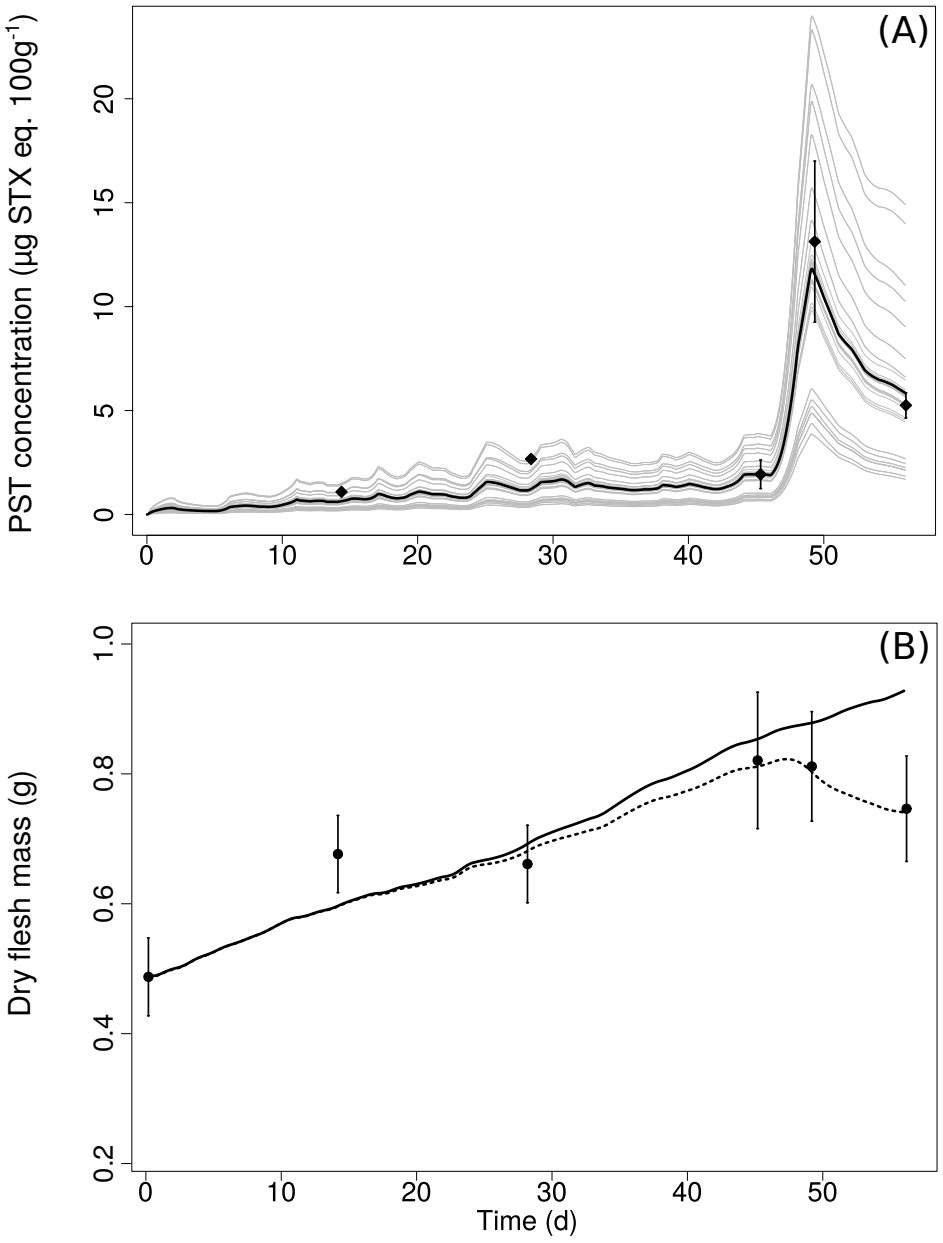

FIGURE 6: Observed (black dots, with vertical error bars as standard deviation) and predicted (lines) toxin concentration (µg STX eq. $100g^{-1}$) in *C. gigas* over time (A), and observed (dots, with vertical error bars as standard deviation) and predicted (lines) dry flesh mass (g) of oysters over time (B) while feeding on a mix of toxic and non-toxic algae (dataset 3). The solid grey (i.e. individual model predictions of 25 individuals) and solid black (mean model prediction of the 25 ind.) lines were obtained by using $[PST]_q$ = 7 µg STX eq. $100g^{-1}$. The dashed line represents the mean of 25 individuals simulated with a value for $[PST]_q$ estimated from these observations (1 µg STX eq. $100g^{-1}$). The starting points correspond to the initial measurements of 25 oysters. ρ_{PST} was adjusted to 0.150 µg STX eq. J^{-1}.

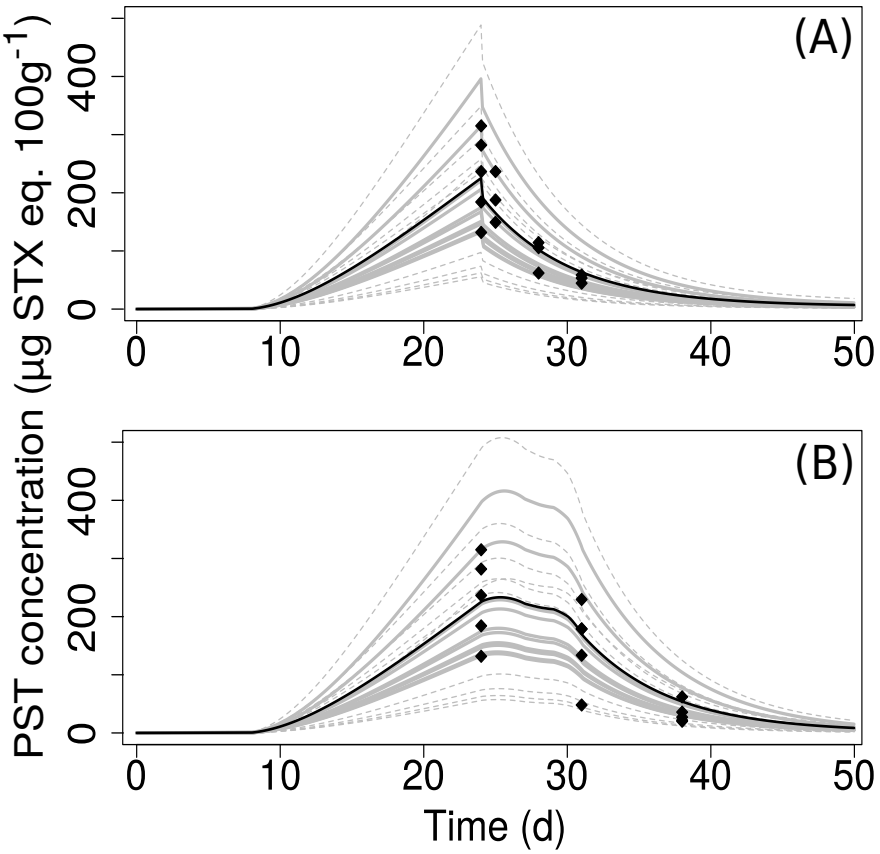

FIGURE 7: Observed (dots) and predicted (lines) concentrations of PST in oysters during a bloom of *A. minutum* in the bay of Brest (field accumulation stage, dataset 4) and after the bloom (laboratory detoxification in filtered seawater starting at day 24, A and at day 31, B). Simulations were run with the DEB-PST model on 20 individuals ($\rho_{PST} = 0.086$ µg STX eq. J^{-1}). Grey dashed lines correspond to individuals with low and high potential of PST accumulation, continuous grey lines indicate individuals with intermediate accumulation potential and black lines refer to the mean of all individuals.

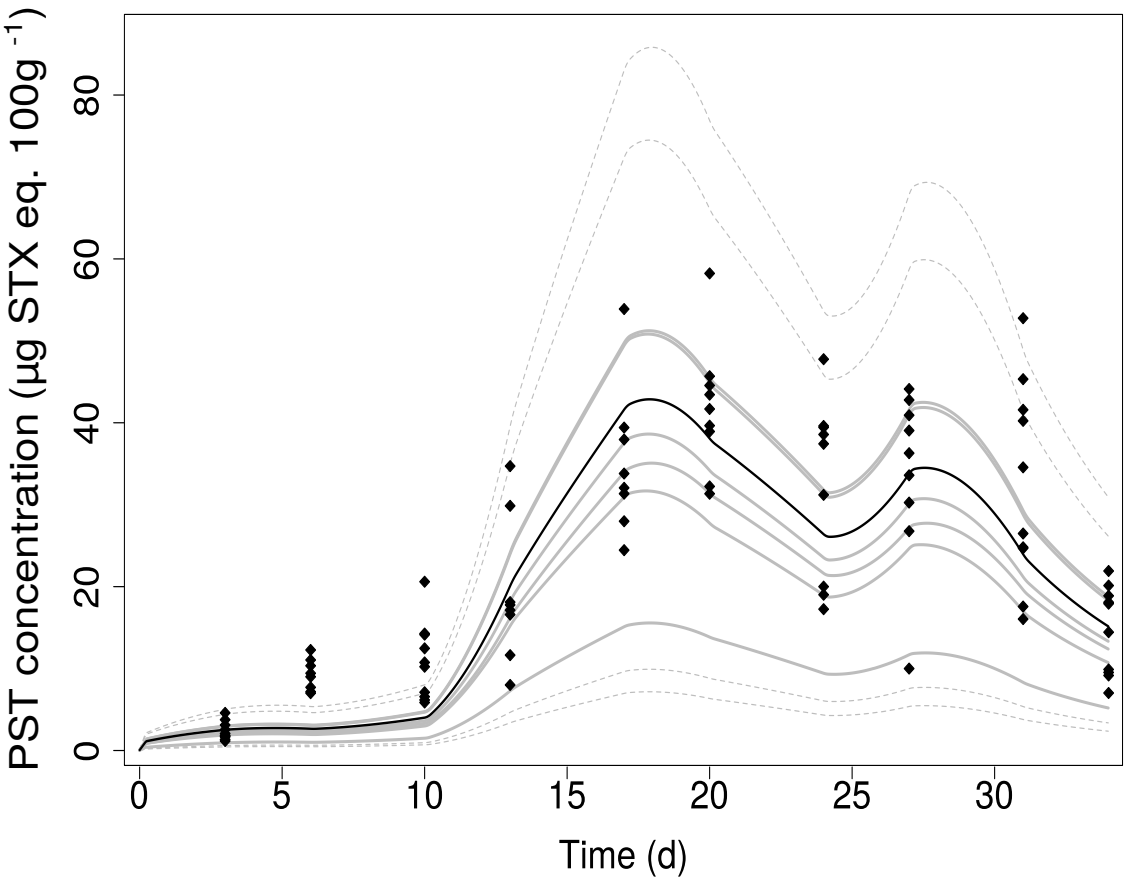

FIGURE 8: Observed (symbols) and predicted (lines) concentrations of PST in oysters transferred in the bay of Brest prior to a bloom of *A. minutum* in 2013 and sampled over 30 days (dataset 4). Simulations were run with the DEB-PST model on 10 individuals ($\rho_{PST} = 0.463$ µg STX eq. J^{-1}). Grey dashed lines correspond to individuals with low and high potential of PST accumulation, continuous grey lines indicate individuals with intermediate accumulation potential and black lines refer to the mean of all individuals.

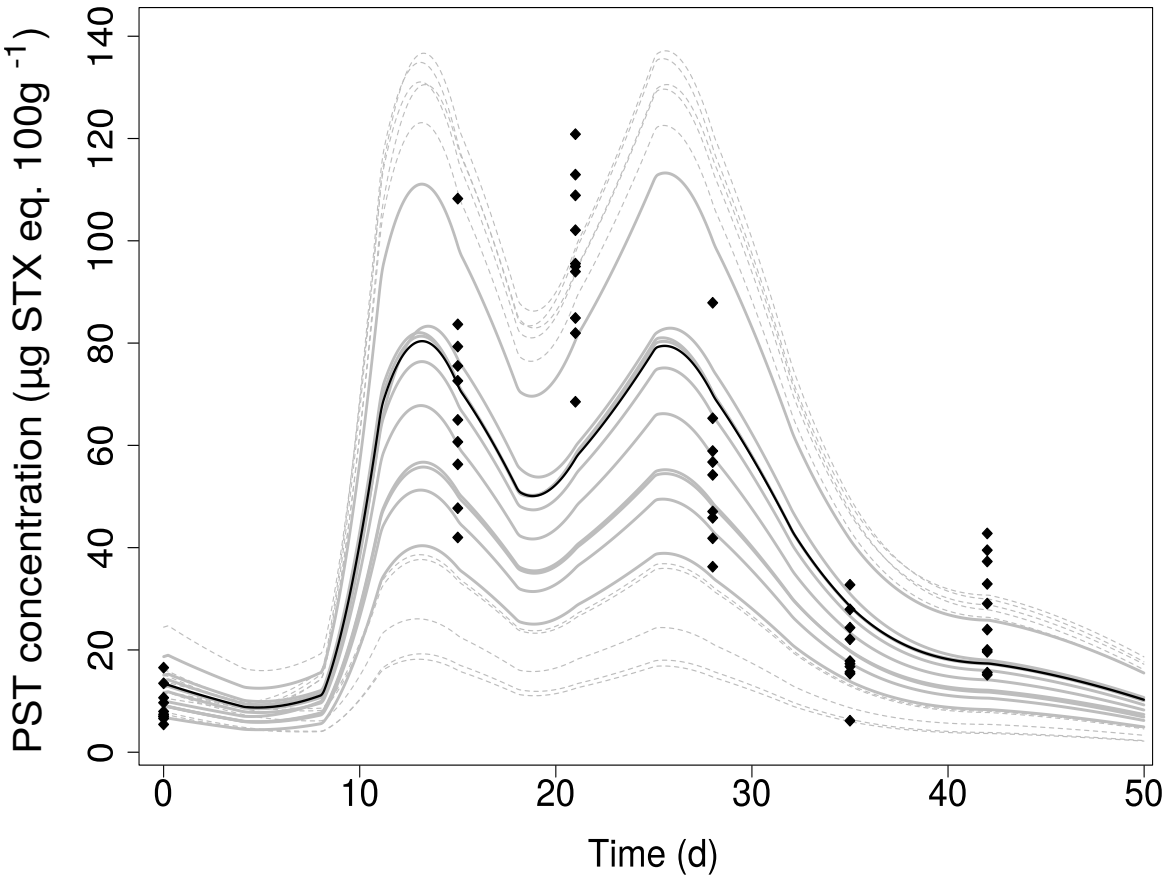

FIGURE 9: Observed (symbols) and predicted (lines) concentrations of PST in oysters transferred in the bay of Brest prior to a bloom of *A. minutum* in 2014 and sampled over 42 days (dataset 4). Simulations were run with the DEB-PST model on 20 individuals ($\rho_{PST} = 0.431$ µg STX eq. J^{-1}). Grey dashed lines correspond to individuals with low and high potential of PST accumulation, continuous grey lines indicate individuals with intermediate accumulation potential and black lines refer to the mean of all individuals.

TABLE 1: Parameters of the DEB-PST model for *Crassostrea gigas*. Symbols, values, units and source of each parameter are given.

Description	Symbol	Value	Unit	References
SU parameters				
Binding rate of non-toxic algae	$\{\dot{F}_{Nm}\}$	12/16/20	$L\,d^{-1}\,cm^{-2}$	Pousse et al. (2017)
Binding rate of toxic algae	$\{\dot{F}_{Tm}\}$	1.5/4/8	$L\,d^{-1}\,cm^{-2}$	Pousse et al. (2017)
Binding rate of non-toxic algae from toxic algae	$\dot{b}_{NT}$	$=\{\dot{F}_{Nm}\}$	$L\,d^{-1}\,cm^{-2}$	Lavaud et al. (2014)
Dry mass of non-toxic algae	M_N	$2.8\ 10^{-11}$	$g_{dw}\,cell^{-1}$	Reynolds (2006)
Dry mass of toxic algae (*A. minutum*)	M_T	$9.4\ 10^{-10}$	$g_{dw}\,cell^{-1}$	Reynolds (2006)
Yield of reserve of non-toxic algae	y_{EN}	0.05	$g_{dw}\,{g_{dw}}^{-1}$	This study
Yield of reserve of toxic algae	y_{ET}	0.005	$g_{dw}\,{g_{dw}}^{-1}$	This study
PST parameters				
STX amount per energy unit in a toxic algae	ρ_{PST}	strain dependent	$\mu g STX\,eq.\,J^{-1}$	This study
Toxin assimilation efficiency	$\kappa_{X_{PST}}$	0.18	$-$	This study
Toxin elimination coefficient	k_{elim}	0.17	d^{-1}	This study
Gut time transit	t_g	$0.135\,V^{1/3} + 0.0125$	d	This study
No-effect concentration	$[PST]_{NEC}$	0.1	$\mu g\,STX\,eq.\,100g^{-1}$	This study
Toxicant stress concentration	$[PST]_q$	7	$\mu g\,STX\,eq.\,100g^{-1}$	This study

TABLE 2: General information of the 4 datasets used in this study either for parameter calibration (datasets 1,2) or for model validation (datasets 3,4).

Dataset	Key features of the experimental conditions	Purposes	Related figures	Sources
Dataset 1	4 trophic conditions for oysters:	**Parameter calibration**		
(Laboratory)	(1) starvation (8 weeks)	κ_{LR}	Fig. 2	
	(2) diet of non-toxic algae (6 weeks)	y_{EN}	Fig. 2	This study
	(3) diet of non-toxic algae and *A. minutum* (6 weeks)	y_{ET}, $\kappa_{X_{PST}}$, k_{elim}, t_g (3,4)	Fig. 3, 5	
	(4) diet of non-toxic algae and *A. minutum* (2 weeks), then starvation (6 weeks)	$[PST]_{NEC}$,$[PST]_q$ (3,4)	Fig. 3, 5	
Dataset 2	Diet of *A. minutum* only for 2 days	**Parameter calibration**		Pousse et al. (2017)
(Laboratory)	*A. minutum* strain identical to dataset 1 synthesizing only PST	$\{\dot{F}_{Tm}\}$, y_{ET}, $\kappa_{X_{PST}}$, t_g	Fig. 4	
Dataset 3	Diet of non-toxic algae and *A. minutum* (8 weeks), peak of *A. minutum* in week 7	**Model validation**		Castrec et al., in prep
(Laboratory)	*A. minutum* strain with PST and BEC*		Fig. 6	
Dataset 4	Oysters transfer in Bay of Brest prior to an *A. minutum* bloom in 2012, 2013, 2014	**Model validation**		This study
(Field)	In 2012, 2 detoxification stages in laboratory after a 25 and 32 days field exposure		Fig. 7, 8, 9	

*BEC = Bioactive Extracellular Compounds

Supplementary material

to

Modelling paralytic shellfish toxins (PST) accumulation in *Crassostrea gigas* by using Dynamic Energy Budgets (DEB)

Émilien Pousse, Jonathan Flye-Sainte-Marie, Marianne Alunno-Bruscia, Hélène Hégaret, Éric Rannou, Laure Pecquerie, Gonçalo M. Marques, Yoann Thomas, Justine Castrec, Caroline Fabioux, Marc Long, Malwenn Lassudrie, Ludovic Hermabessiere, Zouher Amzil, Philippe Soudant, Fred Jean

Appendix 1: DEB-model for the Pacific oyster

Appendix 1.1: Three state variables DEB-model for the Pacific oyster

The core DEB model describing the energy budget of the oyster (*C. gigas*) is the one developed by Bernard et al. (2011) and further updated by Thomas et al. (2016). It is derived from the standard DEB model (Kooijman, 2000). First applications of the oyster-DEB model were published by Pouvreau et al. (2006) and Bourlès et al. (2009). The conceptual scheme of the model is described in Figure S1, the equations are given in Table S1. Parameters signification is given in Table S2 (Appendix 2). This DEB model describes the time change of three state variables: the energy content of reserve, E (J); the structural volume growth, V (cm^3) and the energy allocated to maturity development and reproduction, E_R (J). A fixed fraction (κ) of flux of mobilized reserve ($\dot{p}_C$) is allocated to structural maintenance ($\dot{p}_M$) and growth. Maintenance has priority over growth. The $1 - \kappa$ fraction of mobilized reserve is allocated to maturity or reproduction (E_R) and to maturity maintenance ($\dot{p}_J$, in priority). Bernard et al. (2011) added to the standard DEB model a specific module to detail the energy allocation to gametogenesis, which formulation involves an additional state variables and 4 parameters. In our study, however, this module was removed from the model since the reproduction dynamics was not the focus. The model does not take into account larval life; the transition from juvenile to adult occurs at a fixed size (V_p) according to Kooijman (2000). All metabolic rates are controlled by temperature according to the extensive Arrhenius relationship (Kooijman, 2000, see Eq. 1).

$$c_T = \exp\left\{\frac{T_A}{T_1} - \frac{T_A}{T}\right\}\left(1 + \exp\left\{\frac{T_{AL}}{T_1} - \frac{T_{AL}}{T_L}\right\} + \exp\left\{\frac{T_{AH}}{T_H} - \frac{T_{AH}}{T_1}\right\}\right)$$
$$\left(1 + \exp\left\{\frac{T_{AL}}{T} - \frac{T_{AL}}{T_L}\right\} + \exp\left\{\frac{T_{AH}}{T_H} - \frac{T_{AH}}{T}\right\}\right)^{-1} \quad (1)$$

with c_T the temperature correction parameter applied to each physiological rate of an organism, T_1 the reference temperature (in K) for rates and T_A the Arrhenius temperature (in K). Outside the optimal temperature boundaries (T_L, low boundary and T_H, high boundary), physiological rates drop quickly according the Arrhenius temperature for lower (T_{AL}) and higher (T_{AH}) boundary.

The parameter set is the one used by Thomas et al. (2016), except for the physical length at puberty (L_{wp}). Parameters values are given in Table S2 (Appendix 2).

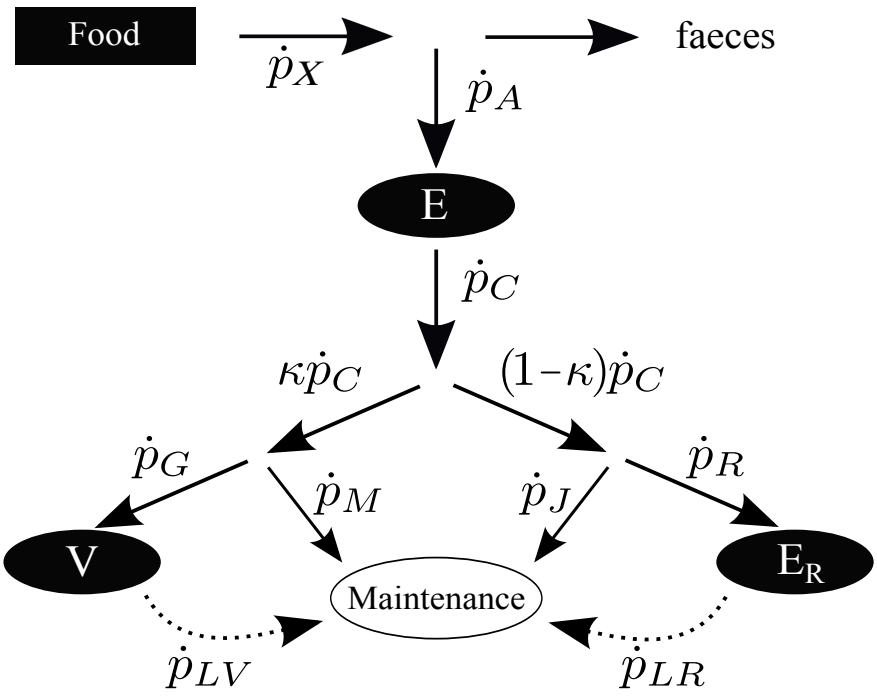

FIGURE S1: Conceptual scheme of the DEB-model modified from Bernard et al. (2011). Energy fluxes are represented by solid arrows. The compartments E, V and E_R (black ellipses) define the energy allocated to the reserves, the structure and the reproduction respectively. White ellipses correspond to maintenance costs (somatic and maturity). In case of starvation, if maintenances costs cannot be fulfilled, energy is firstly obtained from the lysis of E_R ($\dot{p}_{LR}$) then from the lysis of V ($\dot{p}_{LV}$). These fluxes are represented by dotted arrows and detailed in Appendix 1.2.

TABLE S1: Description of all energy fluxes of the DEB model when food resources are sufficient to fulfill maintenance costs. *,denotes fluxes that have been adapted to take into account the Synthesizing Units.

Process	Symbol	Equation
Ingestion*	$\dot{p}_X$	$\{\dot{p}_{Xm}\}V^{2/3}c_T\,(f_N + f_T)$
Assimilation*	$\dot{p}_A$	$\{\dot{p}_{Xm}\}V^{2/3}c_T(f_N\,\kappa_{X_N} + f_T\,\kappa_{X_T})$
Reserve mobilization	$\dot{p}_C$	$[E]c_T\frac{[E_G]\dot{v}V^{2/3}+[\dot{p}_M]V}{\kappa[E]+[E_G]}$ with$[E] = E/V$
Somatic maintenance cost	$\dot{p}_M$	$[\dot{p}_M]V\,c_T$
Growth	$\dot{p}_G$	$\kappa\dot{p}_C - \dot{p}_M$
Maturity maintenance	$\dot{p}_J$	$min(V, V_p)\,\frac{1-\kappa}{\kappa}\,[\dot{p}_M]\,c_T$
Reproduction (when $V \geq V_p$)	$\dot{p}_R$	$(1-\kappa)\dot{p}_C - \dot{p}_J$ else = 0

The energy fluxes allow to calculate the dynamics of the state variables E, V and E_R as follows:

$$\text{Reserve (J)} \quad \frac{dE}{dt} = \dot{p}_A - \dot{p}_C \tag{2}$$

$$\text{Structure } (cm^3) \quad \frac{dV}{dt} = \frac{\dot{p}_G}{[E_G]} \tag{3}$$

$$\text{Reproduction (J)} \quad \frac{dE_R}{dt} = \dot{p}_R \tag{4}$$

Based upon dynamics of the three state variables, the individual wet flesh mass of an oyster is calculated as:

$$W_w = \left(\frac{E + E_R}{\rho_E} + V\,d_v\right)\,\frac{1}{(1-\theta_w)} \tag{5}$$

with the energy content of reserves ρ_E ($J\,{g_{dw}}^{-1}$), the structural density d_V ($g_{dw}\,cm^{-3}$) and the oyster water content (θ_w).

Appendix 1.2: Specific case of starvation conditions

In case of food limitation, when $\dot{p}_C$ is not sufficient to pay somatic maintenance costs ($\dot{p}_M$) and/or maturity maintenance costs ($\dot{p}_J$), the energy is obtained from lysis of the reproduction buffer ($\dot{p}_{LR}$). The compartment E_R is constituted of energy allocated to reproduction and potentially of energy used to develop gonad. It is assumed that the remobilization of energy from the gametes has overheads $(1 - \kappa_{LR}$, with $\kappa_{LR} = 0.79$ estimated from dataset 1; Table S2). When the energy in E_R is totally consumed and thus does not allow to fulfill maintenance costs, the lysis of the structure occurs at the rate $\dot{p}_{LV}$ with $(1 - \kappa_{LV})$ the overheads of structure lysis. The parameter κ_{LV} could not be estimated from the starvation experiment, which did not last long enough to induce the full exhaustion of E_R. Thus, κ_{LV} was arbitrary fixed to 0.79 (Table S2). A scheme describing these fluxes is given in Fig. S1.

In this context, the state variables E, V, E_R are calculated as follows:

When $\kappa\dot{p}_C < \dot{p}_M$:

$$\frac{dE}{dt} = \dot{p}_A - \dot{p}_C \tag{6}$$

if $V \geq V_p$ and $\frac{E_R}{dt} \geq \dot{p}_{LR}$; $\frac{dV}{dt} = 0$ (7)

$$\frac{dE_R}{dt} = -\dot{p}_{LR} \tag{8}$$

$$\text{with} \quad \dot{p}_{LR} = \frac{1}{\kappa_{LR}}(\dot{p}_M - \kappa\dot{p}_C - ((1-\kappa)\dot{p}_C - \dot{p}_J)) \tag{9}$$

else

$$\frac{dE_R}{dt} = 0 \tag{10}$$

$$\frac{dV}{dt} = \frac{-\dot{p}_{LV}}{\rho_V d_V} \tag{11}$$

$$\text{with} \quad \dot{p}_{LV} = \frac{1}{\kappa_{LV}}(\dot{p}_M - \kappa\dot{p}_C - ((1-\kappa)\dot{p}_C - \dot{p}_J))) \tag{12}$$

Appendix 2: Model parameters

Parameters symbols, values, units and sources of the standard model used in this study are presented in Table S2. Except L_{wp}, this entire parameter set has been used in Bernard et al. (2011) and Thomas et al. (2016).

TABLE S2: Parameters of the standard DEB model for *Crassostrea gigas*. Symbols, values, units and source of each parameter are given.

Description	Symbol	Value	Unit	References
Biological parameters				
Shape coefficient	δ_M	0.175	–	van der Veer et al. (2006)
Physical length at puberty	L_{wp}	2.4	cm	This study
Water content	θ_w	0.8	-	This study
Reserve parameters				
Max surface specific ingestion rate	$\{\dot{p}_{Xm}\}$	1 025	$J\,cm^{-2}\,d^{-1}$	Bernard et al. (2011)
Volume specific maintenance cost	$[\dot{p}_{M_0}]$	44	$J\,cm^{-3}\,d^{-1}$	Bernard et al. (2011)
Energy conductance	$\dot{v}$	0.183	$cm\,d^{-1}$	van der Veer et al. (2006)
Assimilation efficiency of non-toxic algae	κ_{X_N}	0.75	–	van der Veer et al. (2006)
Assimilation efficiency of toxic algae	κ_{X_T}	0.65	–	Pousse, unpub. data
Energy content of 1 g of reserve	ρ_E	19 600	$J\,g_{dw}{}^{-1}$	Kooijman (2010)
Molecular weight of reserve	w_E	23.9	$g\,mol^{-1}$	Kooijman (2010)
Yield of reproductive tissue used for maintenance	κ_{LR}	0.79	–	This study
Structure parameters				
Energy fraction allocated to soma	κ	0.45	–	van der Veer et al. (2006)
Volume specific cost for structure	$[E_G]$	3900	$J\,cm^{-3}$	Bernard et al. (2011)
Density of structure	d_V	0.15	$g_{dw}\,cm^{-3}$	Whyte et al. (1990)
Energy content of 1 g of structure	ρ_V	15 600	$J\,g_{dw}{}^{-1}$	Bernard et al. (2011)
Yield of structure tissue used for maintenance	κ_{LV}	0.79	–	This study
Temperature effect				
Arrhenius temperature	T_A	5 800	K	van der Veer et al. (2006)
Reference temperature for rates	T_1	293	K	Bernard et al. (2011)
Lower boundary tolerance range	T_L	281	K	Bourlès et al. (2009)
Upper boundary tolerance range	T_H	300	K	Bourlès et al. (2009)
Arrhenius temperature for lower boundary	T_{AL}	75 000	K	van der Veer et al. (2006)
Arrhenius temperature for upper boundary	T_{AH}	30 000	K	van der Veer et al. (2006)

Appendix 3: Sensitivity analysis

To assess the influence of the parameters calibrated in this study on the growth and the PST accumulation in oysters, a sensitivity analysis was conducted. The sensitivity index was calculated from the following equation (Bodiguel et al., 2009):

$$\mathrm{SI}(\%) = \frac{1}{\mathrm{n}} \sum_{i=1}^{n} \frac{|\hat{y}_i^1 - \hat{y}_i^0|}{\hat{y}_i^0} 100 \tag{13}$$

where n is the number of time steps, $\hat{y}_i^0$ and $\hat{y}_i^1$ are respectively the model predictions (in this case dry flesh mass and PST concentration in oyster) with the calibrated and modified parameter value at time t. Modified value corresponds to -10% or +10% of the calibrated parameter value (see Table 1). The sensitivity index was calculated from model predictions of dataset 1 (condition 3, i.e. diet of non-toxic algae and *A. minutum* for 6 weeks).

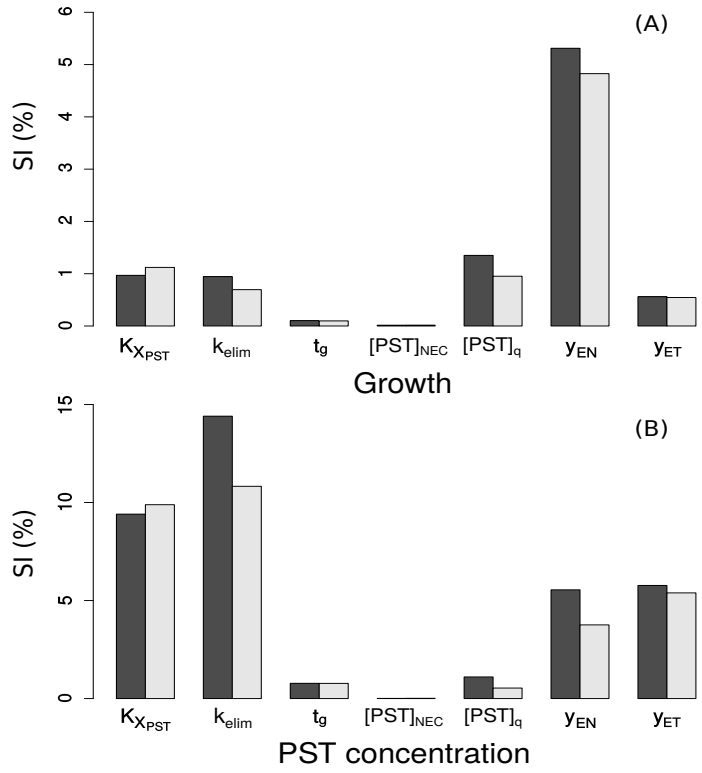

FIGURE S2: Sensitivity index (SI) for growth (A) and PST concentration (B) computed for DEB-PST parameters calibrated in this study. Effects of -10% and +10% variation of parameter values are respectively represented in dark and light grey. The sensitivity analysis was run on model outputs of dataset 1 from condition 3 (diet of non-toxic algae and *A. minutum* for 6 weeks).

Results of the sensitivity analysis on growth predictions show that the yield of reserve of non-toxic algae (y_{EN}) is the most sensitive parameter (Fig. 2, A). Three parameters linked to toxins ($\kappa_{X_{PST}}$, k_{elim}, $[PST]_q$) exhibit a similar influence on growth. Surprisingly, these parameters are more sensitive than the yield of reserve of toxic algae (y_{ET}) which is an energy linked parameter.

Concerning the sensitivity indexes calculated for the PST accumulation predictions (Fig. 2, B), parameters $\kappa_{X_{PST}}$ and k_{elim} lead to an important mean variation of 9.6% and 12.6% predictions in PST concentrations, respectively. It can also be noticed that y_{EN} and y_{ET} affect in a rather similar way (respectively 4.6% and 5.6% in average) the predicted PST concentration, indicating that the impact of non-toxic algae on PST accumulation in oysters are at least as important as the impact of toxic algae. Finally, this analysis shows that the gut time transit (t_g) and the no-effect concentration ($[PST]_{NEC}$) have a weak effect on growth and PST concentration predictions.

Appendix 4: HPLC-FLD measurements of PST

Appendix 4.1: PST profiles in oysters

TABLE S3: Toxin profile (%mol) measured by HPLC-FLD of oysters sampled during 2012, 2013 and 2014 surveys (dataset 4).

Year	dc-GTX3	GTX5	dc-GTX2	GTX3	GTX2	NeoSTX	STX	C1	C2	C3
2012	0.14	1.03	0.46	13.75	24.66	0.68	1.22	26.90	28.93	2.23
2012	0.27	3.29	1.27	14.81	30.49	0.52	0.82	37.94	8.63	1.96
2012	0.22	2.82	1.17	16.82	22.94	1.59	1.12	33.26	9.96	10.10
2012	0.20	6.83	1.01	15.96	24.89	1.46	1.15	36.71	9.27	2.51
2012	0.23	4.86	1.25	13.02	22.55	6.12	0.99	40.40	8.13	2.45
2012	0.24	4.36	1.38	13.87	24.72	4.36	0.90	38.82	8.37	2.99
2012	0.19	4.97	1.07	15.56	21.77	4.42	1.46	38.53	8.80	3.22
2012	0.25	4.45	1.47	13.52	23.34	2.37	1.22	39.15	10.25	3.98
2012	0.20	4.01	1.36	14.17	25.85	2.17	1.24	33.00	10.12	7.87
Mean	0.21	3.68	1.06	17.03	23.94	2.21	1.01	34.06	13.23	3.57
2013	0.00	0.00	0.00	37.90	34.72	0.00	0.00	0.00	0.00	27.38
2013	0.00	0.00	0.00	34.08	16.53	19.61	0.00	0.00	4.24	25.53
2013	0.00	0.00	0.00	41.20	22.11	0.00	0.00	0.00	0.00	36.68
2013	0.37	0.00	0.00	37.64	15.68	0.00	0.00	0.00	11.14	35.17
2013	0.51	0.00	0.00	43.12	16.40	0.00	0.00	0.00	8.18	31.78
2013	0.78	0.00	1.91	30.47	17.52	12.72	0.00	0.00	10.63	25.96
2013	0.00	0.00	0.00	27.90	26.93	0.00	0.00	0.00	19.16	26.02
2013	0.48	0.00	0.00	30.31	14.86	0.00	0.00	0.00	12.40	41.95
2013	0.39	0.00	0.91	32.27	15.09	0.00	0.00	0.00	12.81	38.52
2013	0.29	0.00	0.56	31.49	18.04	0.00	0.00	0.55	21.40	27.67
2013	0.24	0.00	0.66	43.38	11.46	0.00	0.00	0.69	17.47	26.10
2013	0.20	0.00	0.75	32.04	13.82	0.00	1.40	0.87	18.79	32.13
2013	0.29	0.00	1.23	29.31	20.63	0.00	2.52	1.19	19.14	25.69
2013	0.33	5.48	1.60	15.74	33.90	0.00	0.00	1.90	24.66	16.38
2013	0.28	4.60	1.66	18.02	28.86	0.00	0.00	1.69	30.18	14.71
Mean	0,28	0.67	0.62	32.33	20.44	2.16	0.26	0.46	14.01	28.78
2014	0.17	0.00	0.23	23.88	11.40	0.54	0.00	12.25	51.52	0.00
2014	0.24	0.00	0.28	35.35	15.08	0.74	0.00	10.08	38.22	0.00
2014	0.17	0.00	0.27	33.31	14.64	0.62	0.00	12.72	38.27	0.00
2014	0.21	0.00	0.32	29.23	16.75	0.70	0.00	12.86	39.93	0.00
2014	0.19	0.00	0.29	29.84	19.41	0.88	0.00	12.31	37.08	0.00
2014	0.15	0.00	0.22	34.58	15.85	0.65	0.17	11.60	36.77	0.00
Mean	0.19	0.00	0.27	31.03	15.52	0.69	0.03	11.97	40.30	0.00

Appendix 4.2: Relationship between HPLC and ELISA measurements

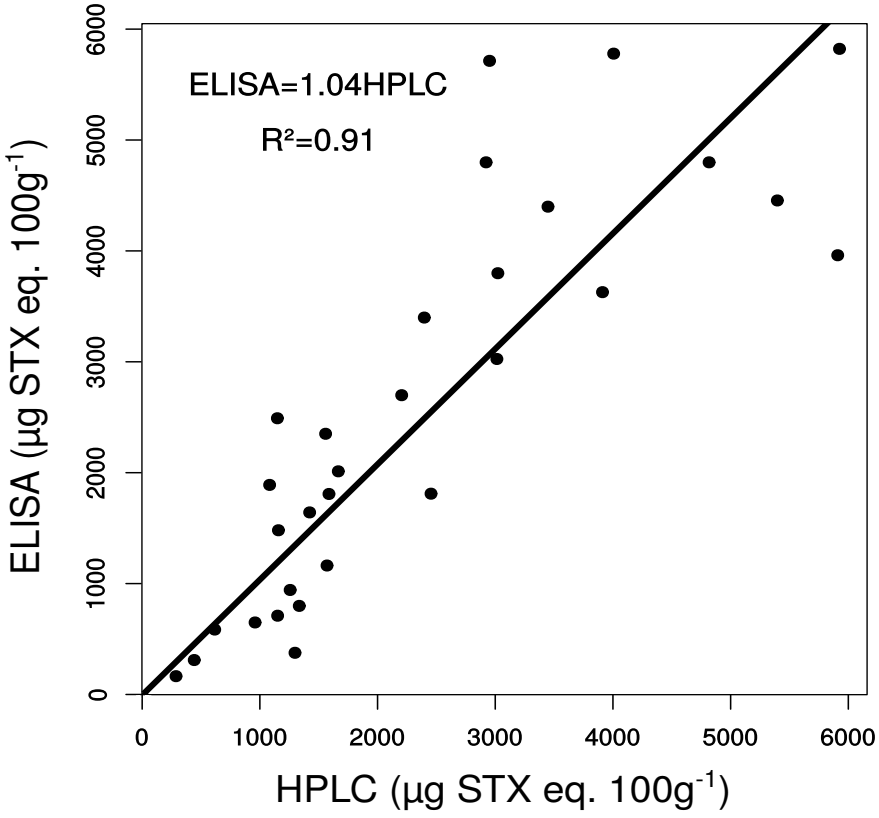

FIGURE S3: PST concentrations of oysters from 2012, 2013 and 2014 surveys (dataset 4) analyzed by ELISA (µg STX eq. $100g^{-1}$) and HPLC-FLD (µg STX eq. $100g^{-1}$) techniques. A linear regression (black line, intercept forced to zero) was applied to these data.

References

Bernard, I., De Kermoysan, G., Pouvreau, S., 2011. Effect of phytoplankton and temperature on the reproduction of the Pacific oyster *Crassostrea gigas* : investigation through DEB theory. J. Sea Res. 66 (4), 349–360.

Bodiguel, X., Maury, O., Mellon-Duval, C., Roupsard, F., Le Guellec, A.-M., Loizeau, V., 2009. A dynamic and mechanistic model of PCB bioaccumulation in the European hake (*Merluccius merluccius*). J. Sea Res. 62 (2), 124–134.

Bourlès, Y., Alunno-Bruscia, M., Pouvreau, S., Tollu, G., Leguay, D., Arnaud, C., Goulletquer, P., Kooijman, S., 2009. Modelling growth and reproduction of the Pacific oyster *Crassostrea gigas* : advances in the oyster-DEB model through application to a coastal pond. J. Sea Res. 62 (2), 62–71.

Kooijman, S. A. L. M., 2000. Dynamic energy and mass budgets in biological systems. Cambridge university press.

Kooijman, S. A. L. M., 2010. Dynamic energy budget theory for metabolic organisation. Cambridge university press.

Pouvreau, S., Bourles, Y., Lefebvre, S., Gangnery, A., Alunno-Bruscia, M., 2006. Application of a dynamic energy budget model to the Pacific oyster, *Crassostrea gigas*, reared under various environmental conditions. J. Sea Res. 56 (2), 156–167.

Thomas, Y., Pouvreau, S., Alunno-Bruscia, M., Barillé, L., Gohin, F., Bryère, P., Gernez, P., 2016. Global change and climate-driven invasion of the Pacific oyster (*Crassostrea gigas*) along European coasts : a bioenergetics modelling approach. J. Biogeogr. 43 (3), 568–579.

van der Veer, H. W., Cardoso, J. F., van der Meer, J., 2006. The estimation of deb parameters for various Northeast Atlantic bivalve species. J. Sea Res. 56 (2), 107–124.

Whyte, J., Englar, J., Carswell, B., 1990. Biochemical composition and energy reserves in *Crassostrea gigas* exposed to different levels of nutrition. Aquaculture 90 (2), 157–172.